
SYNTHESIS AND DESIGN OF SPARSE LINEAR ANTENNA (SLA) ARRAYS

2.1 Context and Background

As discussed in chapter 1, keeping in view the limitation and requirements of active antenna arrays for radar applications and motivated by the aspects of sparse array, author carried out research in this framework. This research would be worthwhile in the frame work of antenna technology for military radar systems. In this chapter, author describes various synthesis approaches for the design of sparse linear antenna (TLA and NUSLA) arrays based on GA and PSO optimization techniques, as part of his Ph.D. research work. This chapter provides studies on TLA and NUSLA arrays with various problems of interest having different objectives.

2.2 Thinned Linear Antenna (TLA) Arrays

2.2.1. Introduction

The study on TLA arrays is broadly divided into four parts as mentioned below. Details of each are described subsequently in different Sub-sections.

- PSL Optimization in 100-element TLA Array at Boresight Using GA
- Optimization of PSL and Maximization of Number of 'OFF' Elements in 100- and 200-element TLA Arrays Using MBC-GA
- PSL Optimization in 100-element TLA Array at Boresight as well as upto $\pm 60^\circ$ Scan Angles Using PSO
- Optimization of PSL, HPBW, and Gain in 100- element TLA Array Using MBC-GA

2.2.1.1. PSLL Optimization in 100-Element TLA Array at Boresight Using GA

The objective of this part of study is to synthesize thinned linear array with reduced peak side lobe level (PSLL). The excitation amplitude is assumed to be constant across all the array elements and genetic algorithm (GA) optimization technique is used to compute the best arrangement of 'ON' and 'OFF' elements corresponding to optimum PSLL. To evaluate the performance of proposed method, a 100-element TLA array with uniform inter-element spacing of 0.5λ is considered. Proposed array parameters are evaluated through numerical simulation and the performance comparison with the previously published results is reported.

2.2.1.2. Optimization of PSLL and Maximization of Number of 'OFF' Elements in 100- and 200-Element TLA Arrays Using MBC-GA

In this part of research work, an innovative approach for the synthesis of uniformly excited thinned linear antenna arrays is proposed, which provides a better solution in terms of reduction in peak side lobe level (PSLL) at less computational cost. The solution achieves design performance with less number of turn 'ON' elements, which reduces the cost as well as weight of the antenna array. An innovative variant of genetic algorithm (GA) designated as modified binary coded genetic algorithm (MBC-GA) is proposed for the synthesis of the arrays. Novel techniques for crossover and mutation operations are investigated to make the proposed MBC-GA optimizer a better efficient synthesis tool as compared to classical GA and other methods reported in literature. The potentiality of the proposed approach is exemplified by numerically analyzing a 100-element thinned linear antenna (TLA) array. Results obtained using the proposed synthesis strategy for the arrays under consideration demonstrate the significant improvement in design performance in terms of PSLL reduction with less number of

turn ‘ON’ elements at less computational complexity over the existing state-of-the-art methods.

The process of thinning of an antenna array makes some of the antenna elements ‘inactive’ in order to achieve the desired elements’ density related to reduced value of PSLR while maintaining other characteristics of antenna array nearly the same as for a fully filled array of identical size [Oliveri *et al.* (2010)]. The advantage gained through array thinning is that the total number of radiating elements is substantially reduced which scales down the array cost, weight and power consumption. Further, it results in simple realization of feed network as all the elements across the array would have equal amplitude excitations [Leeper (1999)], [Pocca (2010)].

Various global optimization techniques such as genetic algorithm (GA) [Goldberg *et al.* (1991), Haupt (1994), Tang *et al.* (1996), Weile *et al.* (1997), and Yan *et al.* (1997), Man *et al.* (1999), Gangwar *et al.* (2015b)], and its variants [Donelli (2004), Chen *et al.* (2006), Mahanti *et al.* (2007), Kadri *et al.* (2010), Cen *et al.* (2012), Zhang *et al.* (2012), Ha *et al.* (2015), and Cheng *et al.* (2016)], improved binary invasive weed optimization (IBIWO) [Liu *et al.* (2014)], Boolean differential evolution (BDE) [Zhang *et al.* (2010)], particle swarm optimization (PSO) and its variants [Deligkaris *et al.* (2009), Donelli *et al.* (2009), Zhang *et al.* (2009), Wang *et al.* (2012), Gangwar *et al.* (2015a), Gangwar *et al.* (2016), and Gangwar *et al.* (2017)], ant colony optimization (ACO) [Oscar *et al.* (2006)], and others [Oliveri *et al.* (2011a)], [Oliveri *et al.* (2011b)] have been successfully employed and proven to be suitable for the synthesis of thinned arrays. In general, capability of optimization algorithms is determined by their solution quality in terms of design performance, computational complexity and stability in solving the problem at hand. Although various techniques including those mentioned in

[Goldberg *et al.* (1991), Haupt (1994), Tang *et al.* (1996), Weile *et al.* (1997), Yan *et al.* (1997), Man *et al.* (1999), Oscar *et al.* (2006), Zhang *et al.* (2010), Wang *et al.* (2012), Liu *et al.* (2014), and Gangwar *et al.* (2015b)] have been employed successfully, but the solution quality obtained through them might not be effective and might have ended up with sub-optimum solution.

To improve the solution quality, several researchers suggested some novel processions in their GA based synthesis techniques including those reported in [Donelli (2004), Chen *et al.* (2006), Kadri *et al.* (2010), Cen *et al.* (2012), Zhang *et al.* (2012), Ha *et al.* (2015), and Cheng *et al.* (2016)]. Ha *et al.* [Ha *et al.* (2015)] proposed modified compact genetic algorithm (M-cGA), which is derived from compact genetic algorithm (cGA) by implementing more than one probability vector. Mahanti *et al.* [Mahanti *et al.* (2007)] used real coded genetic algorithm with elitist strategy. In [Cheng *et al.* (2016)], Cheng *et al.* brought in an improved multi-objective optimization algorithm based on non-dominated sorting GA II (NSGA-II) to meet the thinning requirements of a large planar array with a given filling factor and lowest possible PSL. In this synthesis technique, GA is combined with iterative fast Fourier transform (IFFT) technique to improve the solution quality. Kadri *et al.* [Kadri *et al.* (2010)] introduced fuzzy genetic algorithms (FGAs) in which the control parameters like crossover and mutation probabilities of a standard version of genetic algorithm (SGA) are adjusted using a fuzzy controller (FLC) to achieve good improvement in the thinned array performance. In [Zhang *et al.* (2012)] Zhang *et al.* proposed an orthogonal genetic algorithm (OGA) to optimize the planar thinned array for minimum peak side lobe level in which crossover operator formed by the orthogonal array and the factor analysis is employed to enhance its performance. In addition, many techniques other than GA

including those reported in [Donelli *et al.* (2009), Zhang *et al.* (2009), and Liu *et al.* (2014)] have also shown some furtherance for such purpose. Liu *et al.* [Liu *et al.* (2014)] utilized the adaptive dispersion mechanism to improve the search ability of binary IWO. Donelli *et al.* [Donelli *et al.* (2009)] devised a hybrid approach, which exploits and combines the most attractive feature of PSO and those of a combinatorial method based on the noncyclic difference sets of Hadamard type. Zhang *et al.* [Zhang *et al.* (2009)] proposed a modified PSO where the code resetting of optimal variables was introduced during optimization process while Oliveri *et al.* [Oliveri *et al.* (2011a)] proposed a hybrid approach based on genetic algorithm (GA)-enhanced almost difference set (ADS) to improve the performance. Although advancements in aforesaid state-of-the-art synthesis methods have improved the solution quality, the solution achieved through these methods might not be optimal.

In this research work, a modified binary coded genetic algorithm (MBC-GA) is proposed to enhance the solution quality. Particularly, the MBC-GA is investigated to accomplish following improvements which would make it a more efficient synthesis tool as compared to the existing to state-of-the-art thinning techniques:

- An innovative robust randomization strategy for crossover operation, which ameliorates convergence rate by allowing for adequate amount of randomization and diversity to the solution space
- An unexampled systematic mutation strategy that leads the MBC-GA much dynamism, soundness, and rapidity in attaining desired solution
- Higher computational efficiency

The innovative contents and motivation for the current study differ from the existing state-of-the-art thinning techniques in two main aspects. The first aspect of the

present study is that it provides maximum possible reduction in PSLL with less number of turn 'ON' antenna elements. The second aspect involves the development of MBC-GA technique for the synthesis of thinned arrays, yielding good quality and stable solution (the best possible PSLL in a computationally efficient manner). The distinguishing competency of the proposed method is demonstrated by numerically examining 10×20-element TPA array. Results obtained using the proposed technique are compared with those obtained through the techniques available in literature [Oscar *et al.* (2006), Zhang *et al.* (2010), Wang *et al.* (2012), and Liu *et al.* (2014)]. These results show the superiority of proposed MBC-GA technique. Further, the stability of solution is examined by running several independent trials for the arrays under consideration.

2.2.1.3. PSLL Optimization in 100-Element TLA Array at Boresight as well as upto $\pm 60^\circ$ Scan Angles Using PSO

This part of study presents thinning of a linear array that generates radiation patterns with reduced peak side lobe level (PSLL). Uniform amplitude excitation across all the elements is assumed and particle swarm optimization (PSO) technique is used to estimate the optimum combination of 'ON' and 'OFF' elements corresponding to lowest possible peak SLL. In order to assess and validate the performance of proposed method for thinning of a linear array, an array consisting of 100 sources with uniform inter-element spacing of 0.5λ is considered. Array performance is compared with the results obtained for the arrays in which all the elements are turned 'ON' and with previously published results. The capability of proposed method is further demonstrated for thinning of linear phased array by assuming the array of 100 elements which is steered upto $\pm 60^\circ$ with respect to antenna boresight. The radiation pattern characteristics of the phased array for the specified scan angle are reported and compared with those obtained

at antenna boresight.

Various radiation characteristics of an antenna array such as side lobe level (SLL), half power beam width, directivity and gain can be controlled and optimized by adjusting some of the basic array parameters, which include total number of antenna elements, the spacing between them, their amplitude excitation coefficients and relative phases along with the geometrical configuration of overall array, such as linear, planar, circular, elliptical etc. [Balanis (2005)]. Thinning of an antenna array essentially implies that excitation of some of the elements of the uniformly-spaced or periodic array is made equal to zero in order to obtain desired radiation pattern characteristics. The radiating element connected to auxiliary network is 'turned on' and the one, connected to matched load is 'turned OFF' [Haupt (1994), and Wang et al. (2013)]. Statistical optimization methods, such as Newton, downhill and conjugate gradient methods are not well suited to address the problems associated with thinned antenna array because they can only optimize few continuous problems and could get stuck in local maxima [Mailloux and Cohen (1991)]. Therefore, several evolutionary or probabilistic optimization techniques including immune algorithm (IA) [Jianfeng *et al.* (2008)], simulated annealing (SA) [Trucco (1999)], ant colony optimization [Teruel and Iglesias (2006)], particle swarm optimization [Kennedy and Eberhart (1995), Robinson and Samii (2004), and Wang *et al.* (2012)], and genetic algorithm (GA) [Haupt (1995), Mahanti *et al.* (2007), and Cen *et al.* (2012),] have been devised for thinning of antenna arrays. Algorithms reported in the aforementioned literature have demonstrated the synthesis of thinned linear or planar arrays with respect to antenna boresight and shown pretty good reduction in peak PSL.

The objective of the present research work is to synthesize uniformly-excited thinned linear array with reduced peak side lobe level. A particle swarm optimization

(PSO) technique is proposed to determine the optimal combination of ‘ON’ and ‘OFF’ elements in a linear array that would result in maximum possible reduction in peak SLL. A 100-element uniformly excited thinned linear array is assumed and analysed numerically in order to assess the performance of proposed algorithm in reducing peak side lobe level and results obtained using the proposed algorithm are compared with those available in the literature [Teruel and Iglesias (2006), Mahanti *et al.* (2007), and Wang *et al.* (2012)]. In addition, the problem of thinned linear array synthesis for wide steering angle with respect to antenna boresight is also reported. The performance of proposed technique is demonstrated through the synthesis of 100-element thinned linear array when steered upto $\pm 60^\circ$ with respect to antenna boresight. The radiation pattern characteristics of the array at the specified scan angle are reported and comparison is made with those determined at antenna boresight.

2.2.1.4. Optimization of PSSL, HPBW, and Gain in 100- element TLA Array Using MBC-GA

The objective of this part of study is to synthesize thinned linear array with reduced peak side lobe level (PSSL), narrow half power beam width (HPBW) and improved gain or directivity. The excitation amplitude is assumed to be constant across all the array elements. The MBC-GA optimization technique is used to compute the best arrangement of ‘ON’ and ‘OFF’ elements corresponding to optimum peak SLL, beam width and gain or directivity. Thinning of linear array consisting of 100-elements with uniform inter-element spacing of 0.5λ is considered in order to evaluate the performance of the proposed method. Proposed array parameters are evaluated through numerical simulation and the performance comparison with previously published results is reported.

The optimum values of various radiation parameters of an antenna array such as side lobe level (SLL), half power beam width, directivity and gain can be achieved by properly controlling the number of antenna elements distributed at the aperture. Thinning an antenna array means reducing the number of elements by making amplitude excitation equal to zero for some of the elements of the uniformly-spaced or periodic array. Several stochastic optimization techniques, such as simulated annealing (SA) [Trucco (1999)], immune algorithm (IA) [Jianferg *et al.* (2008)], particle swarm optimization [Kennedy and Eberhart (1995), Robinson and Samii (2004), and Wang *et al.* (2012)], ant colony optimization [Teruel and Iglesias (2006)], and genetic algorithm (GA) [Haupt (1995), Mahanti *et al.* (2007), and Cen *et al.* (2012),] have been used for thinning of antenna arrays. Algorithms reported in aforementioned literature have demonstrated the synthesis of thinned linear or planar arrays by assuming only single parameter to be optimized i.e. reduction of PSL. However, it is necessary to have optimal values of side lobe level, half power beam width and directivity or gain together for any practical application, specifically military radar application.

The objective of the present study is to synthesize uniformly-excited thinned linear array with reduced peak side lobe level, narrow half power beam width and higher gain/ directivity for the fixed length of aperture. A genetic algorithm (GA) optimization technique is proposed to determine the best combination of ‘ON’ and ‘OFF’ elements in 100-element linear array that would result in optimal values of aforesaid radiation parameters. The performance of proposed algorithm in achieving the optimum values of PSL, HPBW and gain or directivity of the array are evaluated and compared with those available in the literature [Haupt (1995) and Teruel and Iglesias (2006)].

2.2.2 Geometrical Configuration and Problem Formulation for TLA Arrays

2.2.2.1. PSLL Optimization in 100-element TLA Array at Boresight Using GA

A general configuration of linear array consisting of $2N$ antenna elements distributed symmetrically along X-axis is shown in Fig. 2-1. For this structure, the total field \vec{E}_{total} radiated at an angle θ can be computed as [Balanis (2005), Gangwar *et al.* (2015a), and Wang *et al.* (2012)]

$$\vec{E}_{\text{total}} = [\vec{E} \text{ (Element at reference)}] \times [\text{Array Factor}(\text{AF}(\theta))] \quad (2.1)$$

where

$$\text{AF}(\theta) = \sum_{n=-N}^N A_n e^{j(n-1)\psi}, \quad \psi = kd\cos\theta + \beta \quad (2.2)$$

β is progressive phase difference between two adjacent elements, \vec{E} (Element at reference) is the radiation pattern of single element which is assumed as $\cos(\theta)$ pattern in this study, A_n is the amplitude excitation of the n^{th} element, k is wave number equal to, $2\pi/\lambda$, λ is free space wavelength, and 'd' is inter-element spacing. In the synthesis of thinned array, the amplitude excitation coefficient A_n is assumed to be '1', if the state of the n^{th} element is 'ON' or 'active', and '0', if the state of the n^{th} element is 'OFF' or 'inactive'.

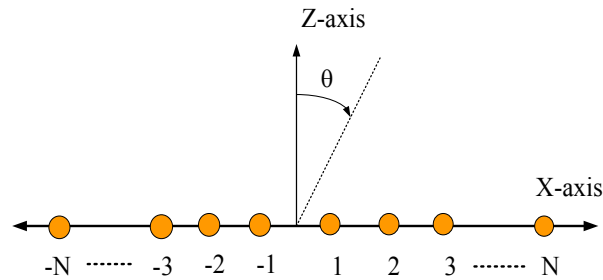


Fig. 2-1: General configuration of a linear array with $2N$ antenna elements.

The fitness function considered in the present study is the normalized maximum side lobe level of the radiation pattern. The normalized maximum side lobe level can be computed using Eq. (2.3).

$$F_{SLL}(A_n) = \max_{\forall \theta \in AR} \left[20 \log \left| \frac{AF(A_n, \theta)}{AF_{max}} \right| \right] \quad (2.3)$$

where AR indicates the angular sector excluding the main beam, and AF_{max} is the maximum value of array factor. Function in Eq.(2.4) reduces during search process.

$$f(A_n) = F_{SLL}(A_n) \quad (2.4)$$

2.2.2.2. Optimization of PSLL and Maximization Number of ‘OFF’ Elements in 100- and 200-element TLA Arrays Using MBC-GA

A general configuration of linear array consisting of $2N$ antenna elements distributed symmetrically along X-axis as shown in Fig. 2-1 is assumed in this study. For this structure, the total field \vec{E}_{total} radiated at an angle θ can be computed using Eq. (2.1).

The fitness function employed in this study is to reduce the peak side lobe level (PSLL) of the array radiation pattern while maintaining the thinning percentage equal to or greater than a fixed value. The normalized minimum side lobe level ($Y_{SLL}(A_n, \theta)$) of the antenna radiation pattern in dB is computed using Eq. (2.5)

$$Y_{SLL}(A_n) = \max_{\forall \theta \in AC} \left[20 \log \left| \frac{AF(A_n, \theta)}{AF_{max}} \right| \right] \quad (2.5)$$

where AC indicates the angular sector excluding the main beam, and AF_{max} is the maximum value of array factor. The thinning percentage (THP) in the thinned array geometry can be formulated as [Gangwar *et al.* (2015a)]:

$$THP = \frac{N_{OFF}}{N_{ON} + N_{OFF}} \times 100 \quad (2.6)$$

where N_{OFF} is total number of ‘OFF’ elements and N_{ON} is total number of ‘ON’ elements in thinned array.

The fitness function given in Eq. (2.7) is adopted during the search process to achieve maximum possible reduction in PSSL under the constraint that the thinning percentage should be equal to or greater than a fixed value.

$$f_{\text{PSSL}}(A_n, \theta) = Y_{\text{SLL}}(A_n, \theta) \mid \text{s.t. } \text{THP}_a \geq \text{THP}_d \quad (2.7)$$

where THP_a is the achieved thinning percentage and THP_d is the desired thinning percentage.

2.2.2.3. PSSL Optimization in 100-element TLA Array at Boresight as well as upto $\pm 60^\circ$ Scan Angles Using PSO

The general configuration of linear antenna array as shown in Fig. 2-1 is considered in this study. The array contains $2N$ elements symmetrically placed about the origin along X-axis. The total field radiated by this array in X-Z plane is calculated using Eq. (2.1).

The fitness function considered in the present study is the normalized maximum side lobe level of the radiation pattern, which is desired to be as low as possible over the scan volume under consideration, is computed using Eq. (2.3).

2.2.2.4. Optimization of PSSL, HPBW, and Gain in 100-element TLA Array Using MBC-GA

The general architecture of linear antenna array as shown in Fig. 2-1 is considered in this study, which consists of $2N$ elements symmetrically placed along X-axis. The expression of total field radiated by this array in X-Z plane is given in Eq. (2.1).

The fitness function considered in the present study is the normalized maximum side lobe level of the radiation pattern. Fitness function given in Eq. (2.3) is desired to be as low as possible under the constraints that $\text{HPBW} \leq$ desired value, and $\text{gain} \geq$ the required value.

2.2.3 Optimization Techniques for the Synthesis of TLA Arrays

2.2.3.1 PSSL Optimization in 100-Element TLA Array at Boresight Using GA

In this synthesis approach, genetic algorithm (GA) as described in section A1.1 (Appendix-A) is used to determine the best configuration of TLA array that would result in minimum possible value of PSSL. Random population consisting of 1,000 chromosomes is generated. GA minimizes the function in Eq (2.4) during optimization.

2.2.3.2 Optimization of PSSL and Maximization of Number of ‘OFF’ Elements in 100- and 200-element TLA Arrays Using MBC-GA

In this study, MBC-GA described in section A1.2 (Appendix-A) is used to determine the best configuration of TLA arrays that would result in lowest possible value of PSSL and maximum number of ‘OFF’ elements. The commencing population of 50 chromosomes are randomly generated wherein each chromosome consists of 100- and 200-genes for 100- and 200-element TLA arrays respectively. MBC-GA minimizes the function given in Eq. (2.7) during optimization.

2.2.3.3 PSSL Optimization in 100-element TLA Array at Boresight as well as upto $\pm 60^\circ$ Scan Angles Using PSO

In this study, PSO as explained in section A2.1 (Appendix-A) is used to determine the best configuration of TLA array that would result in optimal values of PSSL over pre-specified scan volume. The algorithm is started with a swarm of 1000 particles and run over 100 iterations. The fitness function given in Eq. (2.3) is minimized using the PSO algorithm in order to obtain best fitness value.

2.2.3.4 Optimization of PSLL, HPBW, and Gain in 100-Element TLA Array Using MBC-GA

In this study, MBC-GA described in section A1.2 (Appendix-A) is used to determine the best configuration of TLA array that would result in optimal values of PSLL, HPBW and gain. The starting population of 50 chromosomes is randomly generated wherein each chromosome consists of 100- genes. The function in Eq. (2.3) during was minimized during search.

2.2.4 Numerical Analysis, Results and Discussion

In this section, numerical studies of examples under consideration are carried out to examine the effectiveness of various proposed synthesis methods.

2.2.4.1 PSLL Optimization in 100-element TLA Array at Boresight Using GA

In this study, a thinned linear antenna array is considered for optimization which consists of 100 elements symmetrically spaced 0.5λ apart along the X-axis with its centre at the origin. The uniform amplitude excitation coefficient is assumed across all the elements of the array. The algorithm is started with a population of 1000 chromosomes and run over 300 iterations. The fitness function is minimized using the GA algorithm in order to obtain best fitness value i.e. lowest possible PSLL. The optimal arrangement of 'ON' and 'OFF' elements ('ON' = '1', 'OFF' = '0') obtained by aforesaid GA setting is shown in Table 2-1 and the corresponding optimal distribution of the 'ON' and 'OFF' elements at the aperture is depicted in Fig 2-2. The radiation pattern obtained by the GA for this case has a peak side lobe level (PSLL) better than -21.95 dB as shown in Figs. 2-3 and 2-4.

2.2.4.2 Optimization of PSLL and Maximization of Number of ‘OFF’ Elements in 100- and 200-element TLA Arrays Using MBC-GA

2.2.4.2.1 PSLL Optimization and Maximization of Number of ‘OFF’ Elements in 100-element TLA Array

In this study, thinned array configuration of a 100-element linear array symmetrically spaced 0.5λ apart along the X-axis with its centre at the origin, is numerically examined. All the elements in the linear array are excited with equal amplitude and equal phase. During optimization process, the elements at the array boundary may be made inactive which would alter the array size in every iteration. Therefore, to keep the array of fixed size, the boundary element is always kept ‘active’. The fitness function formulated in Eq. (2.7) is minimized to the least value by utilizing MCB-GA synthesis technique. The variations of overall best fitness value and the fitness value averaged over 30 trials with number of iterations are shown in Fig. 2-5, in which optimum values are achieved after around 60 and 100 iterations for overall best PSLL and PSLL averaged over 30 trials respectively. The best PSLL < -23.18 dB and the PSLL < -22.91 dB averaged over 30 trials are obtained through implementation of MCB-GA for the optimum sequence of ‘active’ and ‘inactive’ elements of the TLA array as indexed in Table 2-2. The corresponding distribution of antenna elements is shown in Fig. 2-6.

In order to verify the performance of the MBC-GA, the numerical results for the radiation pattern of the array obtained through the present algorithm are compared with those obtained earlier utilizing RCGA [Mahanti *et al.* (2007)], ACO [Teruel and Iglesias (2006)], and CBPSO [Wang *et al.* (2012)] and these results are presented in Figs. 2-7 and 2-8. Radiation parameters extracted from Figs. 2-7 and 2-8 are tabulated in Table 2-3. It can be observed clearly from Table 2-3 that the best PSLL obtained by the MBC-GA is -23.18 dB, which is 2.62 dB lower than that attained in [Mahanti *et al.*

(2007)], 2.56 dB lower than that achieved in [Teruel and Iglesias (2006)], and 1.89 dB lower than that reported in [Wang *et al.* (2012)]. This is likely because of the reality that the innovative robust randomization strategy for crossover operation and unexampled systematic mutation strategy described in previous section might have provided sufficient amount of randomization and diversity to the solution space which has enabled MBC-GA with rapid convergence (fewer generations) in attaining good quality solution in terms of PSL and computational load. However, methods in [Mahanti *et al.* (2007)], [Teruel and Iglesias (2006)], and [Wang *et al.* (2012)] have taken more generations (as confirmed by Table 2-4) to converge and even got immobilized in local maxima and finally ended up with sub-optimal solution. This may be due to fact that their solutions space would be having insufficient amount of randomization and diversity.

Furthermore, the HPBW and directivity obtained through the MBC-GA synthesis method are almost equal to those reported in the aforementioned literature. However 26% of thinning is accomplished through the presented approach which is greater than 20% in [Teruel and Iglesias (2006)], 22% obtained in [Mahanti *et al.* (2007)], and 24% in [Wang *et al.* (2012)]. This proves that the proposed MBC-GA based synthesis strategy outperforms those reported in [[Teruel and Iglesias (2006)], Mahanti *et al.* (2007)], and [Wang *et al.* (2012)] in terms of attaining best possible reduction in PSL while maintaining HPBW and directivity with less number of turn ‘ON’ antenna elements. In addition to solution quality, computational complexity is also compared which is generally measured in terms of number of fitness function evaluations associated with the problem at hand. The function evaluations involved till the convergence of algorithm, can be calculated as [Haupt (1994)]

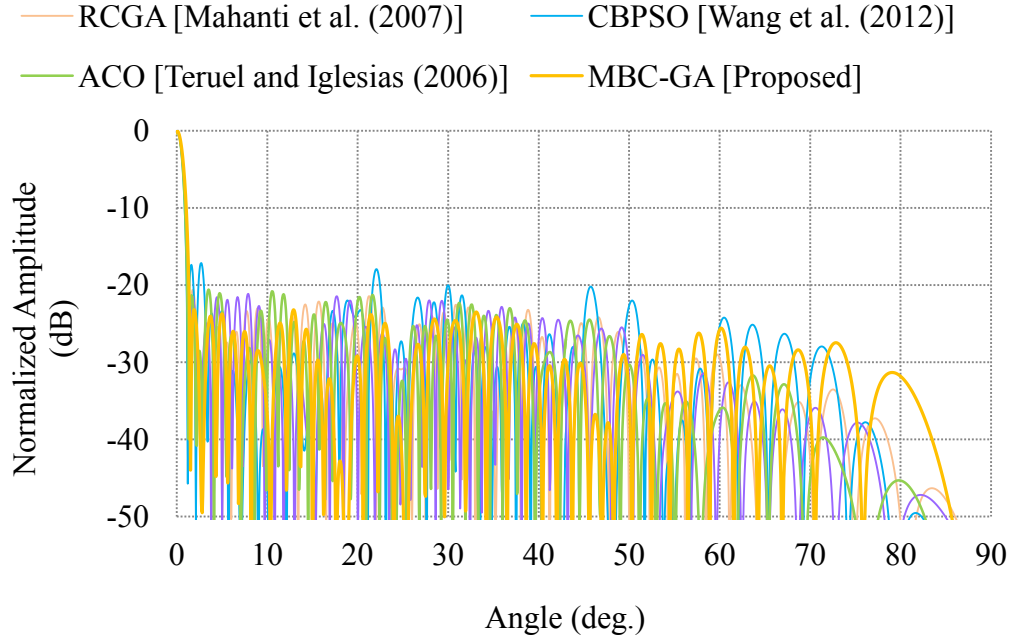


Fig. 2-7: Comparison of radiation patterns of the proposed 100-element TLA array with those of the arrays published in [Teruel and Iglesias (2006)], Mahanti *et al.* (2007)], and [Wang *et al.* (2012)].

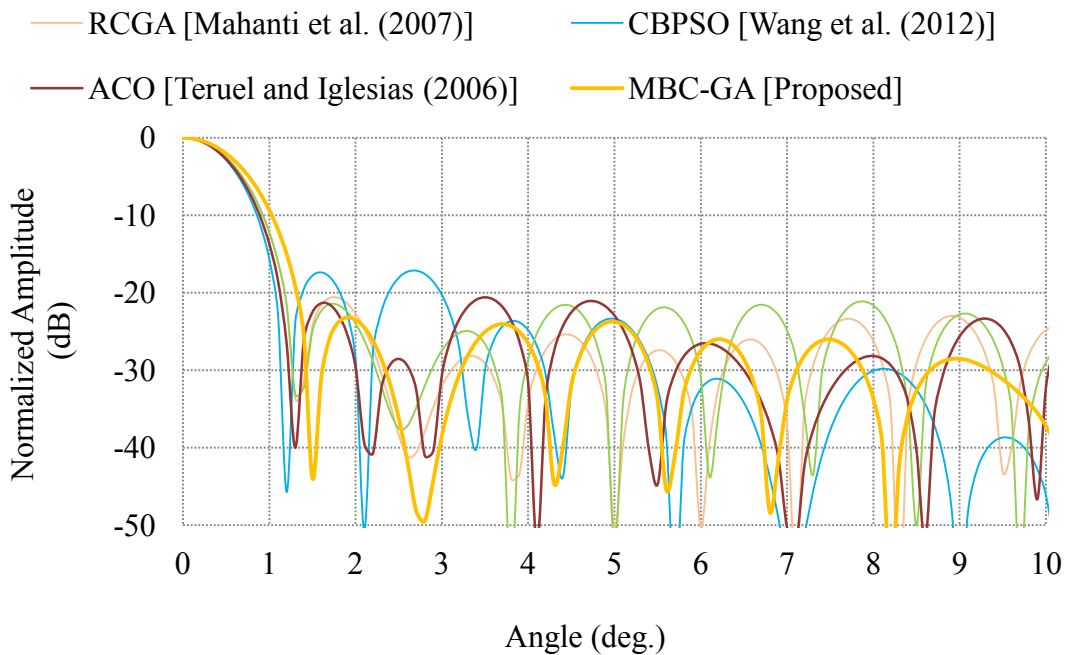


Fig. 2-8: Comparison of radiation patterns of the proposed 100-element TLA array with those of the arrays published in [Teruel and Iglesias (2006)], [Mahanti *et al.* (2007)], and [Wang *et al.* (2012)] in the angular sector ($\theta = 0^0-10^0$).

Table 2-3: Comparison of numerically evaluated results of the proposed 100-element TLA array with those of the arrays reported in [Teruel and Iglesias (2006)], [Mahanti *et al.* (2007)], and [Wang *et al.* (2012)].

Design Parameters	RCGA [Mahanti <i>et al.</i> (2007)]	ACO Teruel and Iglesias (2006)]	CBPSO [Wang <i>et al.</i> (2012)]	MBC-GA [Proposed]
Thinning percentage	22%	20%	24%	26%
Peak SLL (dB)	-20.56	-20.52	-21.29	-23.18
First SLL (dB)	-20.68	-21.55	-17.64	-23.18
HPBW (deg.)	1.1	1.0	1.05	1.18
Directivity (dB)	20.42	20.52	20.49	20.26

Therefore, for a fixed precision (number of angles for array factor computation), the total number of functional evaluations involved till the convergence in the proposed method is compared with those of techniques reported in [Mahanti *et al.* (2007)], and [Wang *et al.* (2012)] and depicted in Table 2-4. It can be noticed from Table 2-4 that computational cost involved in MBC-GA is 82.8% less than that in [Mahanti *et al.* (2007)], and 94.8% less than that in [Wang *et al.* (2012)]. This shows that MBC-GA is computationally more efficient than the techniques reported in [Mahanti *et al.* (2007)], and [Wang *et al.* (2012)]. Apart from MBC-GA capability in terms of attaining best possible reduction in PSL in a computationally efficient fashion, its reliability is also of great concern which is examined by running 30 independent trials and final results are averaged over all the trials. It can be noticed that the best PSL and the PSL averaged over 30 trials are almost same as confirmed by Fig. 2-5. This evidences the stability of proposed MBC-GA optimization algorithm.

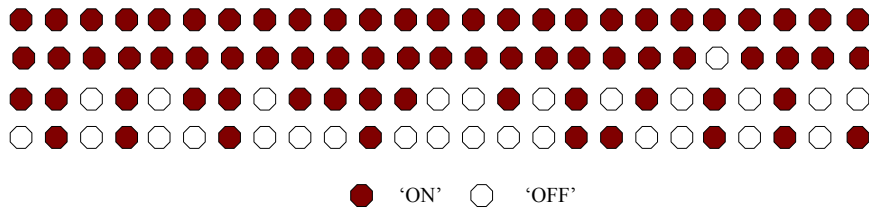


Fig. 2-9: Optimal distribution of half of the 'ON' and 'OFF' elements at the aperture of 200-elements TLA array.

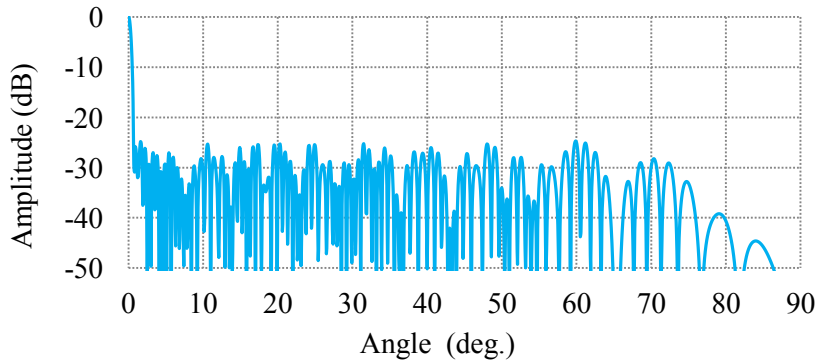


Fig. 2-10: Radiation pattern of the proposed 200-element TLA array.

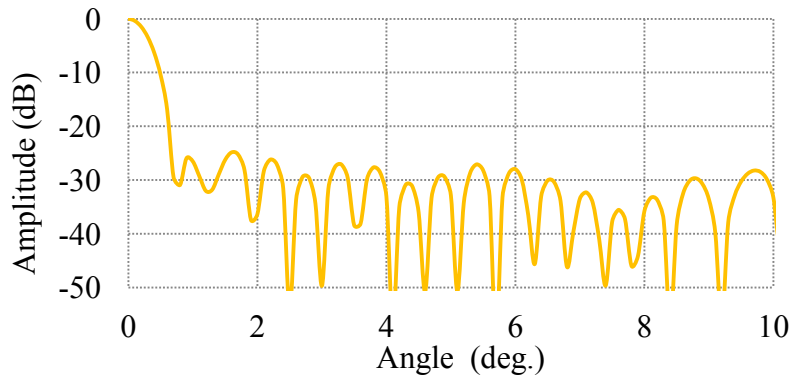


Fig. 2-11: Radiation pattern of the proposed 200-element TLA array in the angular sector ($\theta = 0^0 - 10^0$).

Table 2-6: Comparison of numerically evaluated results of the proposed 200-element TLA array with those of the arrays reported in [Jin and Samii (2007)], [Wang *et al.* (2012a)], and [Ha *et al.* (2016)].

Design parameters	[Ha <i>et al.</i> (2016)]	[Jin and Samii (2007)]	[Wang <i>et al.</i> (2012a)]	MBC-GA [Proposed]
Percentage of thinning	24%	33%	22%	28%
Peak SLL (dB)	-24.3	-19.6	-24.5	-24.71

2.2.4.3 PSL Optimization in 100-element TLA Array at Boresight as well as upto $\pm 60^\circ$ Scan Angles Using PSO

2.2.4.3.1 PSL Optimization at Boresight

In this study, PSO as explained in section A2.1 (Appendix-A) was employed. The numerical factors chosen during optimization are: $c_1 = 0.4$, $c_2 = 0.6$ and r_1 and r_2 are two random numbers between 0 and 1. As per the structure shown in Fig. 2-1, thinning of linear array consisting of 100 sources with $\cos(\theta)$ element pattern was considered in which the elements are symmetrically placed at a uniform spacing of 0.5λ along the X-axis with its centre at the origin. The excitation amplitude is uniform across all the elements of the array and φ_n is equal to zero. Owing to its symmetrical structure, only half of the array is to be optimized.

Initially all the elements of entire array were turned 'ON'. However, while thinning the array, the pair of the centre and the end-elements was switched 'on' in order to keep the size of the array fixed. The algorithm was started with a swarm of 1000 particles and run over 100 iterations. The fitness function given in Eq. (2.3) is minimized using the PSO algorithm in order to obtain best fitness value. Fig. 2-12 shows the variation of best fitness value with number of iterations in the optimization of proposed 100-element thinned linear array with the obtained optimal combination of 'ON' and 'OFF' elements ('ON' = '1', 'OFF' = '0') as listed in Table 2-7 for half of the array. The antenna element distribution is shown in Fig. 2-13. The -22.58 dB PSL in the radiation pattern corresponding to the geometry shown in Table 2-7 is obtained. The results for radiation patterns of the proposed thinned conventional array and of the array with all the elements turned 'ON' are compared in Fig. 2-14.

sacrificing first and peak side lobe levels (SLLs). The first and peak SLLs obtained by the proposed technique are -23.16 dB and -22.58 dB respectively, which are lower than those obtained using algorithms reported in literature [Teruel and Iglesias (2006)], [Mahanti *et al.* (2007)], and [Wang *et al.* (2012b)].

Table 2-8: Comparison of numerically evaluated results for the proposed 100-element TLA array with those of the arrays reported in [Teruel and Iglesias (2006)], [Mahanti *et al.* (2007)], and [Wang *et al.* (2012b)].

Design Parameters	[Mahanti <i>et al.</i> (2007)]	[Teruel and Iglesias (2006)]	[Wang <i>et al.</i> (2012b)]	PSO [Proposed]
Percentage of thinning	22	20	24	26
Peak SLL (dB)	-20.56	-20.52	-21.29	-22.58
First SLL (dB)	-20.59	-21.79	-21.5	-23.16

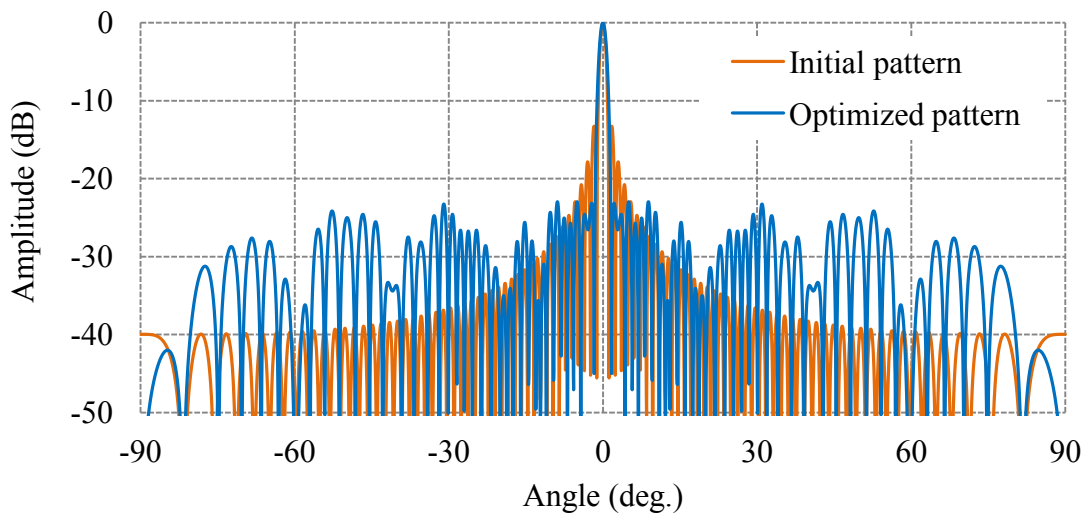


Fig. 2-14: Comparison of radiation pattern of the array with all the elements turned ‘on’ and that of the proposed 100-element TLA array.

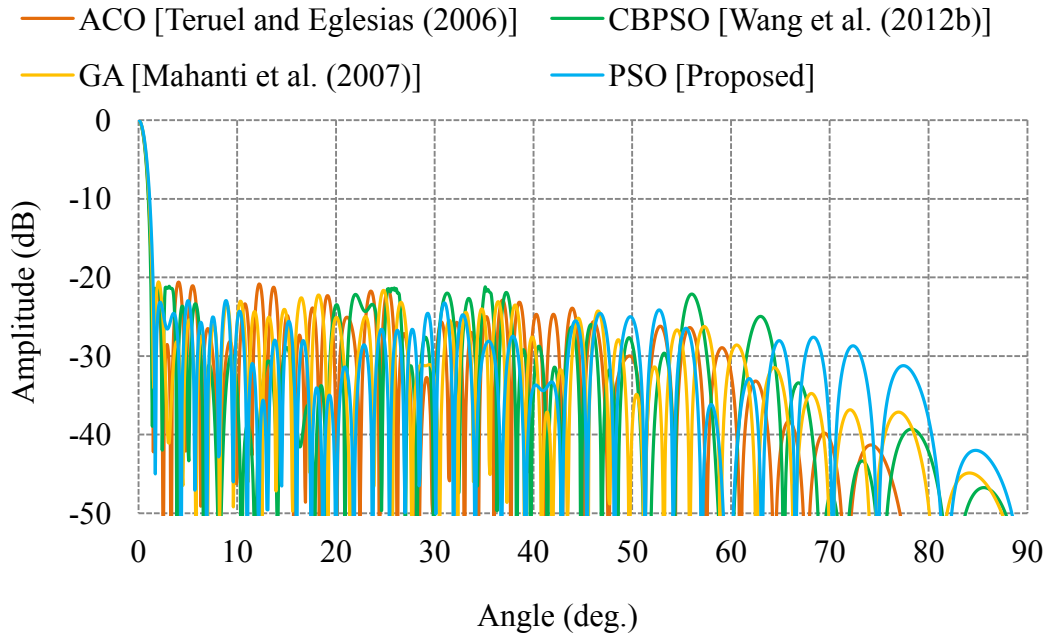


Fig. 2-15: Comparison of radiation pattern of the proposed 100-element TLA array with those of the arrays reported in [Teruel and Iglesias (2006)], [Mahanti *et al.* (2007)], and [Wang *et al.* (2012b)].

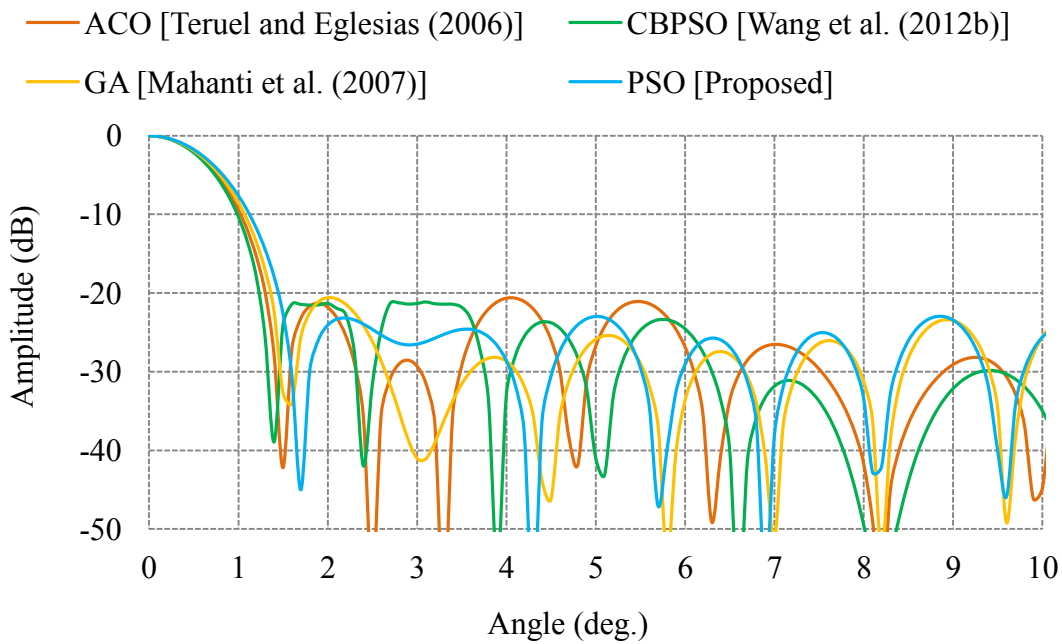


Fig. 2-16: Comparison of radiation pattern of the proposed 100- element TLA array with those of the arrays in [Teruel and Iglesias (2006)], [Mahanti *et al.* (2007)], and [Wang *et al.* (2012b)] in the angular sector ($\theta=0^{\circ}$ - 10°).

2.2.4.3.2 PSLL Optimization up to $\pm 60^\circ$ Scan Angle

A thinned linear phased array consisting of 100 isotropic elements symmetrically spaced 0.5λ apart along the X-axis as per the structure shown in Fig. 2-1 is assumed for numerical analysis at 9.5 GHz.

The maximum angle with respect to boresight that a linear phased array can scan may be calculated using the following expression given in Eq. (2.9) [Balanis (2005)]

$$\theta = \sin^{-1} \left[\frac{d}{\lambda} - 1 \right] \quad (2.9)$$

where θ is the maximum angle that can be steered from antenna boresight, λ is the wavelength, and d is the uniform inter-element spacing. It can be observed from Eq. (2.9) that at $d = \lambda/2$, array can be scanned upto theoretical angle of $\pm 90^\circ$. However, as the inter-element spacing of the array is increased beyond $\lambda/2$, the scan range of the array begins to steadily decrease. In thinned linear array having uniform spacing equal to $\lambda/2$, the average inter-element spacing is always greater than $\lambda/2$ which imposes limitation on array steerability.

In the present study, scan volume upto $\pm 60^\circ$ with respect to the antenna boresight is assumed in order to manifest the performance of proposed method when array is steered upto the above specified angle range. The number of elements (N), uniform inter-element spacing (d), population size and number of iterations are the same as that in the previous 100-element TLA array. The only difference herein is that the aforementioned scan angle is considered as additional parameter in the optimization of phased array. The convergence graph is depicted in Fig. 2-17. The best combination of ‘ON’ and ‘OFF’ elements (‘ON’ = ‘1’, ‘OFF’ = ‘0’) obtained for half of the array is listed in Table 2-9 and the corresponding element distribution at array aperture is shown in Fig. 2-18. The radiation patterns of the proposed TLA phased array are shown in

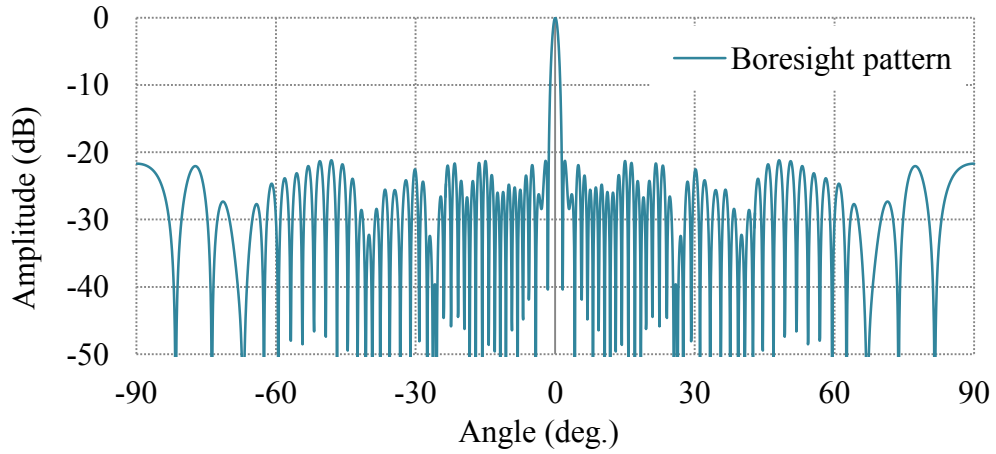


Fig. 2-19: Radiation pattern of the proposed 100-element TLA phased array at boresight ($\theta = 0^\circ$)

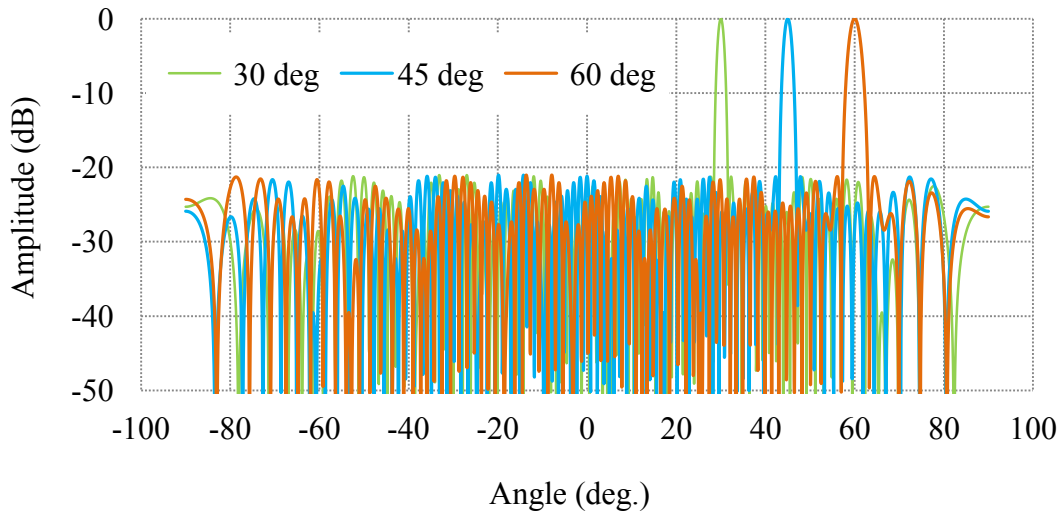


Fig. 2-20: Radiation patterns of the proposed 100-element TLA phased array at scan angles of $\theta = 30^\circ$, 45° , and 60° with respect to antenna boresight.

Table 2-10: Results for the proposed 100-element TLA phased array at boresight and at scan angles of 30° , 45° and 60° away from boresight.

Array parameters	boresight ($\theta = 0^\circ$)	Beam scan to ($\theta = 30^\circ$)	Beam scan to ($\theta = 45^\circ$)	Beam scan to ($\theta = 60^\circ$)
Peak SLL (dB)	< -21.25	< -21.20	< -21.10	< -21.04
First SLL (dB)	< -21.29	< -21.25	< -21.2	< -21.23
HPBW (deg.)	1.19	1.46	1.78	2.08
Directivity (dB)	20.12	19.5	18.7	16.8

2.2.4.4 Optimization of PSL, HPBW, and Gain in 100-element TLA Array Using MBC-GA

Thinning of linear array consisting of 100 sources having $\cos(\theta)$ element pattern and symmetrically placed at a uniform spacing of 0.5λ along the X-axis with its centre at the origin is assumed. The amplitude excitation coefficient is considered uniform across all the elements of the array and phase coefficient (φ_n) is equal to zero. Due to its symmetrical structure, only half of the array is being optimized.

The pair of the centre and the end-elements was switched 'ON' in order to keep the size of the array fixed. The algorithm was started with a population of 10,000 chromosomes and iterated over 100 times. The fitness function given in Eq. (2.3) was minimized using the GA in order to obtain best fitness value. The best fitness values over iterations are shown in Fig. 2-22. The PSL of - 21.57 dB was obtained by the GA with best combination of 'ON' and 'OFF' elements ('ON' = '1', 'OFF' = '0') as listed in Table 2-11 and antenna element distribution at array aperture in Fig. 2-21 for half of the array. The comparison of radiation pattern as shown in Figs. 2-23 and 2-24 of the antenna array using the proposed GA technique is made with those obtained using GA [Haupt (1995)] and ACO [Teruel and Iglesias (2006)] in order to affirm its performance.

The radiation parameters obtained by the aforesaid algorithms and the proposed one are given in Table 2-12. It can be noticed from Figs. 2-23 and 2-24 and Table 2-12 that 26 % thinning percentage obtained by the proposed GA is more than 22% and 20% achieved in [Haupt (1995)] and [Teruel and Iglesias (2006)] respectively without sacrificing any other radiation characteristic of the array. The first and peak SLLs of - 23.6 dB and -21.57 dB respectively have been obtained by the proposed technique

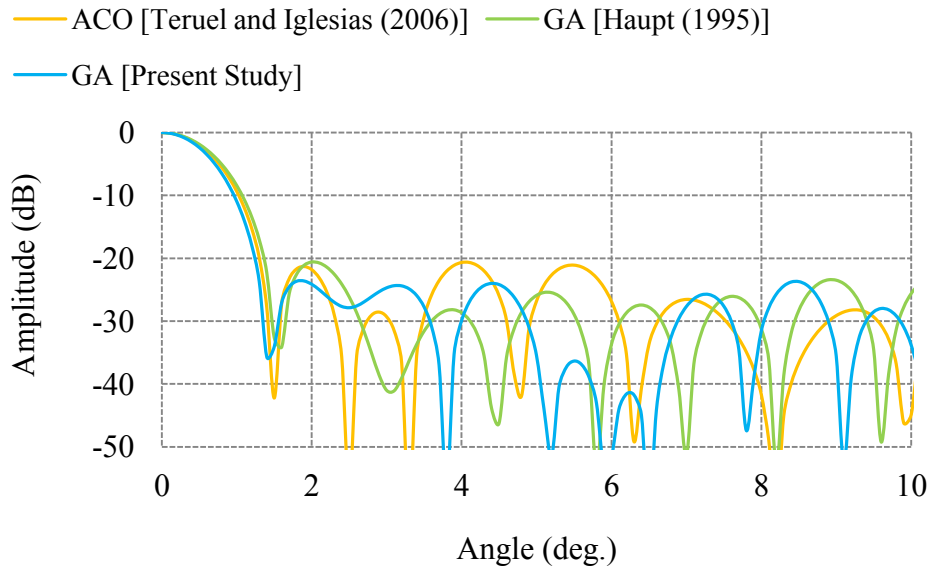


Fig. 2-24: Comparison of radiation patterns of the proposed 100-element TLA array with those of the arrays in [Haupt (1995)], and [Teruel and Iglesias (2006)] in the angular sector ($\theta = 0^{\circ}$ - 10°).

Table 2-12: Comparison of numerically evaluated results for the proposed 100-element TLA array with those of the arrays reported in [Haupt (1995)], and [Teruel and Iglesias (2006)].

Design parameters	ACO [Teruel and Iglesias (2006)]	GA [Haupt (1995)]	GA [Present study]
Percentage of thinning	20	22	26
Peak SLL (dB)	- 20.52	- 20.56	- 21.57
First SLL (dB)	- 21.79	- 20.59	- 23.6
HPBW (deg.)	1.15	1.23	1.08
Directivity (dB)	19.8	19.68	20.16

2.3 Non-uniformly Spaced Linear Antenna (NUSLA) Arrays

2.3.1 Introduction

The study on NUSLA arrays is broadly divided into the following five parts:

- PSL Optimization in 24-element NUSLA Array at Boresight Using GA
- PSL Optimization in 16-and 32-elements NUSLA Arrays by Devising Optimum Elements' Density Using IW-PSO
- PSL Optimization at Boresight as well as upto $\pm 30^\circ$ Scan Angles in 16-element NUSLA Array Using PSO
- Optimization of PSL in Uniformly Excited and Amplitude Weighted 36-element NUSLA Array Using PSO
- EM Simulation and Experimental Validation of 24-element NUSLA Array

The details of each part is described subsequently in different sub-sections

2.3.1.1 PSL Optimization in 24-element NUSLA Array at Boresight Using GA

This study presents synthesis of non-uniformly spaced linear antenna (NUSLA) array with reduced peak side lobe level (PSL). Excitation amplitude is assumed to be constant across all the array elements and the inter-element spacing is kept in the specified range of 0.5λ - 1.5λ . A global optimization algorithm (genetic algorithm) is proposed to compute the optimum arrangement of inter-element spacings corresponding to lowest possible PSL. To validate the effectiveness of the proposed method, an example of NUSLA array with 24-element is analysed numerically. The obtained results are compared with those using uniform element's spacing and with other published approaches for similar design examples. Additionally, the effect of mutual coupling among array elements on the performance of NUSLA array is investigated

through an extensive EM simulation study using commercial HFSS/CST software by considering M-shaped patch radiating elements. The EM simulated pattern for the proposed NUSLA array is compared with that of numerically computed ones.

Tapering of element spacing of an antenna array in the field of array synthesis has attracted the attention of engineers in recent times owing to its advantages, such as offering better side lobe level without any amplitude tapering, late onset of grating lobes, less mutual coupling and simple design of radiating elements. Various optimization techniques have been devised to estimate the optimum inter-element spacing in NUSLA array. In the past, global optimization techniques including genetic algorithm (GA) [Haupt (1995), Chen *et al.* (2006), and Cen *et al.* (2012)], particle swarm optimization (PSO) [Khodier and Christodoulou (2005), Goudos *et al.* (2010)], differential evolution algorithms (DE) [Kurup *et al.* (2003)], iterative algorithms (IA) [Fuchs *et al.* (2012)] and firefly algorithm (FA) [Zaman and Matin (2012)], have been implemented to design NUSLA array for various applications. Most of them [Haupt (1995)], [Chen *et al.* (2006)], [Goudos *et al.* (2010)], and [Fuchs *et al.* (2012)] have not considered the practical aspects of the array and predicted well the characteristics of NUSLA array through numerical study only by assuming isotropic antennas as elementary radiators. Little work [Oraizi and Fallahpour (2008)], [Bencivenni *et al.* (2015)], has been done in the aforesaid area where both theoretical and practical aspects of antenna array design are considered.

The objective of the present study is to consider both theoretical and practical aspects in the synthesis of NUSLA array to overcome the afore-said limitations. To demonstrate the performance of proposed method, NUSLA array with 24 equally excited elements is analysed and its results are reported.

2.3.1.2 PSLL Optimization in 16-and 32-elements NUSLA Arrays by Devising Optimum Elements' Density Using IW-PSO

In this part of study, a simple, effective and computationally efficient approach for the synthesis of uniformly excited NUSLA arrays is proposed. The proposed approach deals with determination of optimum elements' density at the aperture which empowers the synthesis technique with flexibility and increased search competency in attaining maximum possible reduction in PSLL. In the present study, Inertia-weight particle swarm optimization (IW-PSO) algorithm is employed for the synthesis of NUSLA arrays. Numerical analysis on 16-and 32-elements linear arrays is carried out to evidence the effectiveness of proposed approach. The numerical results obtained through the proposed technique are compared with those employing other techniques available in the literature which reveals that the proposed scheme outperforms other schemes and offers great flexibility as well as enhances the global search ability of IW-PSO algorithm in achieving lowest possible PSLL at reduced computational effort.

Synthesis of non-uniformly spaced antenna (NUSA) arrays has been a demanding field over the past several decades. In the past, some global and analytical optimization techniques including those reported in [Tomiyasu (1991), Khodier and Christodoulou (2005), Chen *et al.* (2006), Goudos *et al.* (2010), Lin *et al.* (2010), Goudos *et al.* (2011), Oliveri and Massa (2011), Lin *et al.* (2012), Oliveri *et al.* (2012), Sartori *et al.* (2013), Zhang *et al.* (2013), and Gangwar *et al.* (2015b)] have become more popular for synthesis of NUSA arrays. Particle swarm optimization (PSO) algorithm [Khodier and Christodoulou (2005)], genetic algorithm (GA) [Chen *et al.* (2006)], and Differential evolution algorithm (DEA) [Lin *et al.* (2010)] have been utilized by researchers for such purpose. In this framework, the synthesis methodologies are often-times devised in

terms of PSLL reduction problem, which is solved by appropriately varying the spacing between equally excited elements over the pre-specified intervals.

Synthesis techniques reported in [Tomiyasu (1991)], [Zhang *et al.* (2013)], and [Gangwar *et al.* (2015b)] have been utilized to solve aforementioned problem and to achieve reasonably good reduction in PSLL. The geometrical configurations of elements obtained through these methods demonstrate that some percentages (30% in [Tomiyasu (1991)], 60% in [Zhang *et al.* (2013)], and 66% in [Gangwar *et al.* (2015b)]) of total number of elements in the array are unequally spaced elements towards the edges while the central region elements are equally spaced at the pre-specified minimum value. It appears that only some percentage of elements in the array is sufficient enough to be considered for optimization rather than all array elements. The effectiveness of such synthesis techniques is not only related to the reasonably good estimation of the PSLL but also to the computational capability. The computational complexity is correlated with the number of functional evaluations required to converge. For a given precision, the functional evaluation grows exponentially with the number of optimization variables [Sartori *et al.* (2013)]. This increases computational complexity of the algorithm. Consequently, the development of efficient algorithm is of great interest. Several approaches including those in [Oliveri and Massa (2011)], and [Sartori *et al.* (2013)] have been proposed in the literature to overcome this limitation, wherein Sartori *et al.* in [Sartori *et al.* (2013)] proposed hybridization of an analytical thinning technique based on almost difference sets (ADSs) and a convex programming (CP) strategy while Oliveri and Massa in [Oliveri and Massa (2011)] have used Bayesian compressive sampling (BCS) technique to improve synthesis effectiveness in terms of array performance and computational efficiency.

In this study, a simple, effective, and computationally efficient approach competing with the existing synthesis methods is proposed. The aforementioned percentages of unequally spaced elements i.e. 30% in [Tomiyasu (1991)], 60% in [Zhang *et al.* (2013)], and 66% in [Gangwar *et al.* (2015b)] may not be optimum for attaining maximum possible reduction in PSSL at less computational cost and these algorithms might have landed up with sub-optimum solutions. Keeping in view this point, the author felt the need to devise an efficient synthesis approach by estimating optimum elements' density at the aperture of NUSLA arrays. The proposed approach deals with IW-PSO based synthesis technique for estimating the optimum inter-element spacings within the prescribed intervals in a computationally efficient fashion.

The present study is intended to devise a mathematical relation to approximate the optimum elements' density (optimum percentage of unequally spaced elements as a function of total number of elements) at the aperture of NUSLA arrays. This optimum percentage of unequally spaced elements is employed as an input parameter in IW-PSO algorithm during synthesis process. The proposed approach is expected to offer substantial amount of tractability in the search for an optimum solution as well as it enhances the global search ability of IW-PSO algorithm in conforming to maximum possible reduction in PSSL at less computational cost. In order to observe distinguishing ability and potentiality in terms of performance and design efficiency of the proposed scheme, 16-and 32-element NUSLA arrays are numerically analysed and the results are compared with those obtained through the techniques reported in [Chen *et al.* (2006)], [Lin *et al.* (2010)], [Goudos *et al.* (2010), and Goudos *et al.* (2011)] , [Lin *et al.* (2012)], and [Zhang *et al.* (2013)].

2.3.1.3 PSLL Optimization at Boresight as well as upto $\pm 30^\circ$ Scan Angles in 16-element NUSLA Array Using PSO

An efficient technique for synthesizing NUSLA array is proposed for reducing the peak side lobe level (PSLL) while steering the main beam over the pre-specified scan angles. All the elements in antenna array are assumed to have constant amplitude and phase excitations, whereas elements' spacings are varied in the range $0.5\lambda - 1.5\lambda$. Particle swarm optimization (PSO) algorithm is utilized to determine optimum combination of elements' spacings corresponding to better design efficiency in terms of reduction in PSLL not only at boresight but also at different scan angles. NUSLA arrays present a particular challenge of grating lobes because of average elements' spacings greater than $\lambda/2$. In this study, an attempt is made to overcome this limitation by appropriately determining the range of elements' spacing. A 16-element NUSLA array is chosen for optimisation and results obtained through the proposed method are verified against the uniformly spaced array at 30° scan angle.

The aperiodic placement of uniformly excited antenna elements in arrays enables one to obtain lower PSLL, narrow half power beam width (HPBW), higher gain or directivity and reduces the number of elements for a specified aperture size [Haupt (2010)]. A lot of research effort has been made to suppress the PSLL by optimizing inter-element spacings while providing uniform excitation across all the elements [Harrington (1961), Hodjat and Horanessian (1978), Yu (1997), and Bae *et al.* (2003)]. The optimization of PSLL by the researchers using afore-mentioned techniques is not considered over the scan volume of the array but they have presented good numerical results at the boresight of the antenna array.

However, in electronically scanned radar, unless arrays are optimized over the pre-specified scan volume, grating lobes will appear in antenna visible region. This is

the critical problem, which needs to be addressed at both synthesis and design levels. Very few optimization techniques including those listed in [Haupt (2010)], and [Gangwar *et al.* (2015a)] have been utilized to synthesize the array in order to overcome aforesaid limitation.

The main objective of this study is to consider the scanning aspects during synthesis of NUSLA array and synthesize it for low PSLL not only at antenna boresight but also over the pre-specified scan volume. This is very tough problem since average inter-element spacing is more than λ and also the radiated far field does not linearly depend on the inter-element spacings. PSO is utilized to determine the optimum arrangement of unequally spaced elements corresponding to low PSLL at antenna boresight as well over whole scan volume without appearance of grating lobes.

A 16-element NUSLA array is assumed to assess and verify the performance of proposed method in which inter-element spacing in the range 0.5λ - 1.5λ , constant amplitude excitation, and 0° and 30° scan angles are taken into consideration. The numerical results obtained through the proposed method are compared with a uniformly spaced array of the same size analysed at afore-said scan angles. Proposed method based on PSO is expected to be very efficient in terms of its performance to design the NUSLA arrays for electronically scanned radar systems.

2.3.1.4 Optimization of PSLL in Uniformly Excited and Amplitude Weighted 36-element NUSLA Array Using PSO

In this part of study, a new synthesis strategy for sparse arrays, which provides very low peak side lobe level (PSLL) along with narrow and highly directive main beam for a given aperture size is proposed. In the present strategy, particle swarm optimization (PSO) is employed to jointly optimize the spacing and amplitude excitation of the small

number of elements near the edges rather than total number of elements in the array in a combined manner to simulate required current distribution at the aperture corresponding to lowest possible SLL. A 36-element NUSLA array is theoretically modelled and examined. The computed results show substantial improvement in terms of PSLL as compared with the previously reported results and with those for uniformly spaced Taylor tapered array of similar size.

The aperiodic placement of uniformly excited antenna elements in NUSLA arrays enables one to obtain lower PSLL, narrow half power beam width (HPBW), higher gain or directivity and reduces the number of elements for a specified aperture size [Haupt (2010)]. A lot of research effort has been made to suppress PSLL by optimizing inter-element spacings alone (SO) while providing uniform excitation across all the elements [Chen *et al.* (2006), Goudos *et al.* (2010), Zhang *et al.* (2011) and Gangwar *et al.* (2017)]. The maximum reduction of PSLL achieved by these techniques is of the order of -20 to -22 dB. However, it is preferable for radar application to design an antenna array with very low SLL (< -30 dB) to minimize interference from other objects. This amount of reduction in PSLL is difficult to achieve using the aforementioned techniques. This may be due to the fact that the radiated far field does not linearly depend on the inter-element spacings.

Several solutions including those reported in [Kurup *et al.* (2003), Lin *et al.* (2010), and Cen *et al.* (2012)] have been proposed to reduce PSLL by considering both the spacing-phase (SP) synthesis [Kurup *et al.* (2003), Lin *et al.* (2010)] and spacing-amplitude (SA) synthesis [Cen *et al.* (2012)]. In these methods, researchers have jointly adjusted the positions and amplitude/phase excitations of all the elements in the array and achieved pretty good reduction in PSLL. However, to simulate variable elements' density over the aperture corresponding to lowest possible PSLL and higher aperture

efficiency, the inner elements should have equal spacings/excitations and the edge elements should have unequal spacings/excitations. This means that if the number of edge elements is properly selected, it would result in maximum reduction of PSLR while maintaining narrow and highly directive main beam especially when array size is very large. Additionally, this also reduces the number of variables for computation.

In the present study, an attempt is made to simulate the required current distribution at antenna aperture corresponding to lowest possible PSLR, narrow and highly directive main beam by applying PSO to find the optimum number of edge elements and their spacings and amplitude excitations in a combined manner. The 36-element NUSLA array is analysed and its parameters are determined and results are compared with those obtained using the previously reported methods and those employing Taylor-tapered uniformly spaced array of similar size. The results show that present strategy (adjusting spacings/excitations of only optimum number of edge elements) is very effective in minimizing PSLR while maintaining narrow and highly directive main beam at reduced computational cost.

2.3.2 Geometrical Configuration and Problem Formulation for NUSLA Arrays

2.3.2.1 PSLR Optimization in 24-element NUSLA Array at Boresight Using GA

A general structure of NUSLA array as shown in Fig. 2-25 with $2N$ elements placed symmetrically along X-axis is considered for this study. The expression of the total field radiated from this array in X-Z plane is expressed by Eq. (2.10) [Zaman and Matin (2012)]

$$\vec{E}_{\text{total}} = [\vec{E} \text{ (Element at reference)}] \times [\text{Array Factor(AF}(\theta))] \quad (2.10)$$

$$AF(\theta) = \sum_{n=-N}^N A_n \exp \left[j \left(k \sum_{i=1}^n d_i \cos(\theta) + \varphi_n \right) \right] \quad (2.11)$$

$$x_n = \sum_{i=1}^n d_i \text{ for } n \geq 1 \quad (2.12)$$

where \vec{E} (Element at reference) is radiation pattern of individual element, $AF(\theta)$ is array factor, A_n is the amplitude of n^{th} element (= '1' for uniform excitation), N is the total number of elements in half of the array (= 12 in the present study), k is the wave number = $2\pi / \lambda$, λ is the wave length, θ is the main beam direction from Z-axis, φ_n progressive phase difference, x_n is distance between 1st and n^{th} elements, and d_i is the inter-element spacing

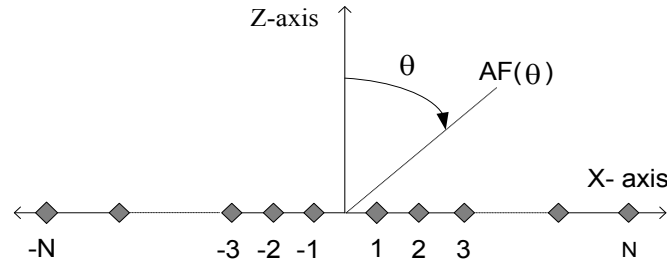


Fig. 2-25: General structure of the NUSLA array with 2N elements

between $(i-1)^{\text{th}}$ and i^{th} antenna elements having the constraint $0.5\lambda \leq d_i \leq 1.5\lambda$. The element positions in the proposed array satisfy the following constraints:

$$\left. \begin{array}{l} x_i - x_{i-1} \geq d_{min} \\ x_i - x_{i-1} \leq d_{max} \end{array} \right\}, \quad 0 \leq i \leq N - 1 \quad (2.13)$$

where d_{min} and d_{max} are the minimum and maximum inter-element spacings respectively.

An objective of the present synthesis is to minimize the peak SLL of NUSLA arrays by optimally computing the inter-element spacing vector $D = [d_1 \ d_2 \ d_3 \ d_4 \ \dots \ d_n]$, subject to given design specifications and constraints.

The fitness function for evaluating PSLL can be defined as

$$F_{SLL}(D) = \max_{\forall \theta \in S} \left[20 \log \left| \frac{AF(D, \theta)}{AF_{max}} \right| \right] \quad (2.14)$$

where S denotes the angular region excluding the main beam, and AF_{max} is the maximum value of array factor. In Eq. (2.14), PSLL is evaluated in dB and is used to reduce it during the optimization.

2.3.2.2 PSLL Optimization in 16-and 32-elements NUSLA Arrays by Devising Optimum Elements' Density Using IW-PSO

A geometrical configuration of unequally spaced linear array is shown in Fig. 2-25 with $2N$ sources placed symmetrically along X-axis and centred at the origin is assumed in this study. The total field radiated by this array in X-Z plane is expressed by Eq. (2.10)

The objective function considered in the present study is the normalized peak side lobe level of the far field pattern. Best fitness value is lowest possible value of PSLL. The objective is to go for best fitness value i.e. to maximize reduction in PSLL using the proposed algorithm. The normalized maximum side lobe level of the antenna array can be calculated using (2.14). The optimization procedure involves searching for the optimal solution of elements' density distribution $D = [d_1, d_2, \dots, d_N]$ which could minimize $F_{SLL}(D)$ in (2.14).

2.3.2.3 PSLL Optimization at Boresight as well as upto $\pm 30^\circ$ Scan Angles in 16-element NUSLA Array Using PSO

The geometrical configuration of the NUSLA array as shown in Fig. 2-25 with $2N$ sources placed symmetrically along X-axis which is centered at the origin is considered

for this study. The total field radiated by this array in X-Z plane is expressed by Eq. (2.10).

The aim of the present synthesis is to minimize PSLL over pre-specified scan volume and at the same time keeping the main lobe to have narrow HPBW and high directivity for given size of aperture. The fitness function for evaluating PSLL can be defined by Eq. (2.14) which is reduced during optimization.

2.3.2.4 Optimization of PSLL in Uniformly Excited and Amplitude Weighted 36-element NUSLA Array Using PSO

The general structure of symmetrical linear array consisting of $2N$ -elements as shown in Fig. 2-25 is considered for this study. The total far-field radiated from this array can be calculated by Eq. (2.10).

The aim of the present synthesis is to minimize PSLL and at the same time keep the main lobe to have narrow HPBW and high directivity for a given size of aperture by computing the optimum inter-element spacings with the constraints $0.5\lambda \leq d_i \leq 1.5\lambda$, and uniform amplitude excitation. The fitness function, which depends upon both inter-element spacing and amplitude excitation can be defined by Eq. (2.15)

$$F_{SLL}(D, A) = \max_{\forall \theta \in AR} \left[20 \log \left| \frac{AF(D, A, \theta, \phi)}{AF_{max}} \right| \right] \quad (2.15)$$

$$f(D, A) = F_{PSLL}(D, A, \theta) |_{\phi=0^\circ} \quad (2.16)$$

where AR denotes the angular region excluding the main beam, and AF_{max} is the maximum value of array factor. Fitness function given in Eq. (2.16) reduces during optimization.

2.3.3 Optimization Techniques for the Synthesis of NUSLA Arrays

2.3.3.1 PSLL Optimization in 24-element NUSLA Array at Boresight Using GA

In this synthesis approach, GA as described in section A1.1 (Appendix- A) is used to determine the best configuration of NUSLA array that would result in minimum possible value of PSLL. Random population of 1,000 chromosomes and 16 genes are randomly generated within the variable inter-element spacings over the range 0.5λ - 1.5λ . GA minimizes the function in Eq. (2.14) during optimization.

2.3.3.2 PSLL Optimization in 16-and 32-elements NUSLA Arrays by Devising Optimum Elements' Density Using IW-PSO

The IW-PSO algorithm as explained in section A2.2 (Appendix- A) [Khodier and Christodoulou (2005)] is employed to solve the NUSLA array problem formulated in Eq. (2.14). The algorithm is started with a swarm of 1000 particles and run over 250 iterations. The fitness function given in Eq. (2.14) is minimized using the IW-PSO algorithm in order to obtain best fitness value.

2.3.3.3 PSLL Optimization at Boresight as well as upto $\pm 30^\circ$ Scan Angles in 16-element NUSLA Array Using PSO

PSO as explained in section A2.1 (Appendix-A) is employed to determine the best configuration of NUSLA array that would result in optimal values of PSLL over pre-specified scan volume. The algorithm is started with a swarm of 1000 particles. The fitness function given in Eq. (2.14) is minimized using the PSO algorithm in order to obtain best fitness value.

2.3.3.4 Optimization of PSLL in Uniformly Excited and Amplitude Weighted 36-element NUSLA Array Using PSO

In the present study, PSO explained in section A2.1 (Appendix-A) is applied to find an optimum inter-element spacings and amplitude excitation coefficients by minimizing the fitness function given in Eq. (2.16). A set of inter-element spacings and excitation coefficients represents a particle and combination of particles is called as swarm.

2.3.4 Numerical Analysis, Results and Discussion

2.3.4.1 PSLL Optimization in 24-Element NUSLA Array at Boresight Using GA

GA was used to determine the optimum inter-element spacing vector $D = [d_1 \ d_2 \ d_3 \ d_4 \ \dots \ d_n]$ which minimizes the $F_{SLL}(D)$ in Eq. (2.14). GA and its variants [Haupt (1995), Chen *et al.* (2006), and Cen *et al.* (2012)] are ideally suited for the synthesis of NUSLA arrays, because they own an intrinsic flexibility to nonlinear problems. The performance of the proposed method is demonstrated by analysing a NUSLA array with 24 equally excited elements. The results were obtained by using a population of 1,000 chromosomes, wherein each chromosome consists of 16 variables to compute. Comparison of design parameters for the proposed 24-element NUSLA array with those for 32-element uniformly spaced array and published results in [Caratelli and Vigano (2011)] and [Goudos *et al.* (2010)] is depicted in Table 2-13.

The algorithm was run 50 times to obtain the optimum arrangements of inter-element spacing. Fig. 2-26 shows the convergence of the PSLL value versus the number of iterations. It can be seen from the Fig. 2-26 that the fitness function value reaches its minimum possible value of -22 dB within 10 iterations. The arrangement of the best inter-element spacing for half of the array obtained with the aforementioned GA

settings is indexed in Table 2-14 and corresponding radiation pattern is depicted in Fig. 2-27. The array parameters evaluated using CLPSO [Goudos *et al.* (2010)] and analytical Technique [Caratelli and Vigano (2011)] are compared with those obtained by the proposed method. The results are illustrated in Table 2-35. It can be observed from Table 2-35 that the PSL is -22 dB, which is 0.33 dB lower than the best PSL obtained in [Goudos *et al.* (2010)] and 2 dB lower than that in [Caratelli and Vigano (2011)]. This demonstrates that proposed method outperforms the synthesis techniques described in [Goudos *et al.* (2010)] and [Caratelli and Vigano (2011)].

Table 2-13: Comparison of design constraints for the proposed NUSLA array with those for 32-element uniformly spaced array and published results in [Goudos *et al.* (2010)] and [Caratelli and Vigano (2011)].

Design parameters	Uniformly spaced array	Analytical Technique [Caratelli and Vigano (2011)]	CLPSO [Goudos <i>et al.</i> (2010)]	GA [Proposed]
d_{\min}	0.5λ	0.34λ	0.47λ	0.5λ
d_{\max}	0.5λ	1.0λ	1.0λ	1.5λ
L	15.7λ	9.72	15.96λ	15.85λ

Table 2-14: Geometry of the best array obtained for half of the proposed 24-element NUSLA array elements.

Element Number (n)	Inter-element spacing (d_i) normalized to λ	Element Number (n)	Inter-element spacing (d_i) normalized to λ
1	0.25	7	0.54
2	0.50	8	0.70
3	0.50	9	0.84
4	0.50	10	0.92
5	0.59	11	0.91
6	0.51	12	1.16

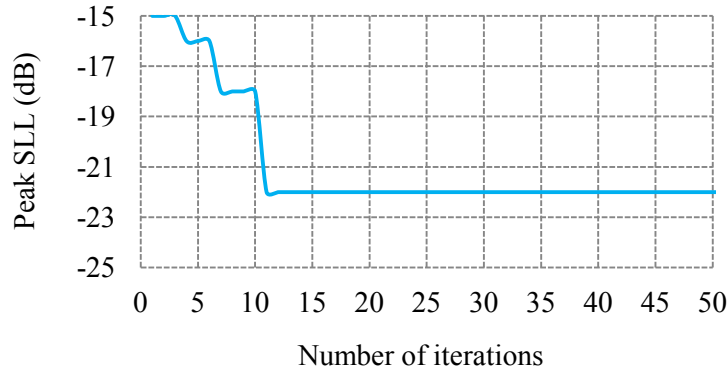


Fig. 2-26: Variation of PSL with number of iterations in the optimization of the proposed 24-element NUSLA array.

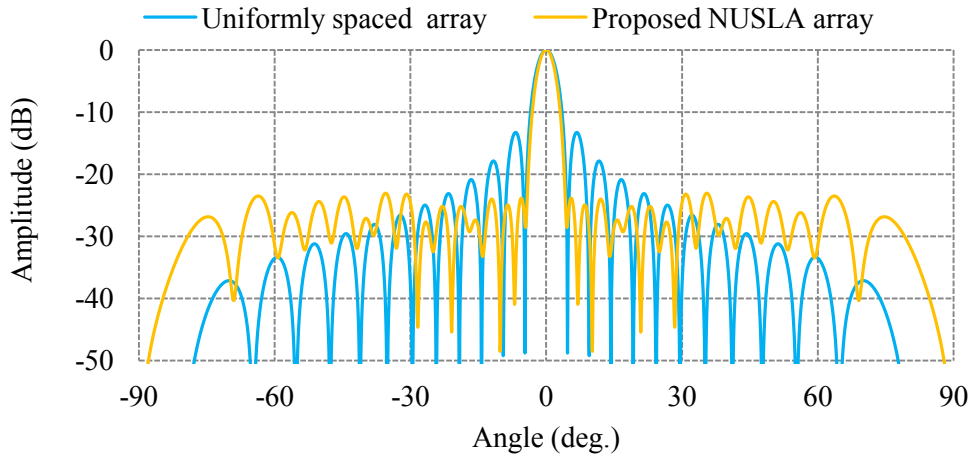


Fig. 2-27: Comparison of numerically evaluated radiation patterns of the proposed 24 -element NUSLA array with that of the 32-element uniformly spaced array in $\phi = 0^\circ$ plane.

Table 2-15: Comparison of numerically evaluated results for the proposed NUSLA array with those of uniformly spaced array and published literature in [Goudos *et al.* (2010)] and [Caratelli and Vigano (2011)].

Parameters	Uniformly spaced array	Analytical Technique [Caratelli and Vigano (2011)]	CLPSO [Goudos <i>et al.</i> (2010)]	GA [Proposed]
Peak SLL (dB)	<-13.2	<- 20	<- 21.63	<-22
HPBW (deg.)	3.49	5.66	3.34	3.4
Directivity (dB)	15.2	-	-	15.3

2.3.4.2 PSLL Optimization in 16-and 32-elements NUSLA Arrays by Devising Optimum Elements' Density Using IW-PSO

In general, antenna elements in the NUSLA arrays are distributed as shown in Fig. 2-28 where they are equally spaced in the central region and unequally spaced towards the edges. Thus, it is necessary to investigate the optimal number of unequally spaced elements of the NUSLA arrays to provide flexibility and enhance the global search ability of the available optimization algorithms.

In this study, it is tried to find out optimum number of unequally spaced elements in NUSLA array in terms of the percentage of total number of elements as given below.

$$\text{Percentage of unequally spaced elements} = \frac{N_{USE}}{N_{ESE} + N_{USE}} \times 100 \quad (2.17)$$

where N_{USE} and N_{ESE} are number of unequally and equally spaced elements respectively, and $(N_{USE} + N_{ESE})$ are total number of elements in NUSLA array. IW-PSO synthesis technique was utilized to simulate optimum distribution of elements' density at the aperture corresponding to lowest possible PSLL for several NUSLA arrays of varying sizes. The robustness was asserted by computing the PSLL several hundred times for each NUSLA array. The resultant data was collected for the arrays of differing sizes and a mathematical relation as given below in Eq. (2-18) is derived through curve fitting of the data collected by total enumeration to approximate the optimum percentage of unequally spaced elements as a function of total number of elements for NUSLA arrays composed of 8 to 64 elements. The associated design curve is plotted in Fig. 2-29.

$$OUSEs = \begin{cases} 100 & \text{for } N_T < 8 \\ K_1 - 21.1 \times \log_e(N_T) & \text{for } 8 \leq N_T \leq 64 \end{cases} \quad (2.18)$$

where $OUSAEs$ is the optimum percentage of unequally spaced elements, K_1 is a constant equal to 122, and N_T is total number of elements in NUSLA array.

It is apparent that Eq. (2.18) will remain accurate for the NUSLA arrays having size varying from 8 to 64 elements. However, it performs with full accuracy for NUSLA arrays of size in the aforementioned range. It is anticipated that a fair degree of accuracy will be asserted for the arrays consisting of elements upto ~ 100 in number. Obtaining data for arrays larger than 64 elements is exceedingly time consuming. Consequently, it is reasonably intemperate to discover the extent to which the equation will remain applicable.

The variations of PSLL with percentage of unequally spaced elements for 16-and 32-element NUSLA arrays are depicted in Fig. 2-30. It is apparent from Fig. 2-30 that PSLL is degraded for each array if the percentage is less or more than the optimum one as approximated using Eq. (2.18). This is probably due to the fact that when the percentage is less than optimum one, optimization algorithm has got less degrees of freedom to lower the PSLL. As percentage is increased beyond the optimum, the complexity increases and optimization algorithm may end up with sub-optimal solution.

The IW-PSO algorithm as outlined in the previous section is illustrated by examining two examples of NUSLA arrays consisting of 16-and 32-uniformly excited elements. The algorithm parameters c_1 and c_2 were set to values of 1 and 3, $r_{1,i}$ and $r_{2,i}$ were set to values of 0.4 and 0.6, inertia weight parameter (ω) was initially set to 0.99 and decreased linearly during the iteration process, and a population size of 1000 particles was considered. The algorithm was iterated 250 times. The central region elements were fixed at equal spacing (d_{min}) of 0.5λ and either side edge element spacings were varied over the range $d_{min} - d_{max}$ i.e. $0.5\lambda - 1.5\lambda$.

In first example consisting of 16-elements, optimum percentage of unequally spaced elements was chosen to be 62.5 % of total number of elements as devised in Eq. (2.18).

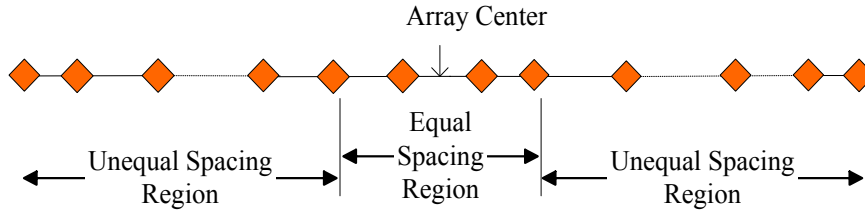


Fig. 2-28: General distribution of antenna elements at the aperture of an NUSLA array.

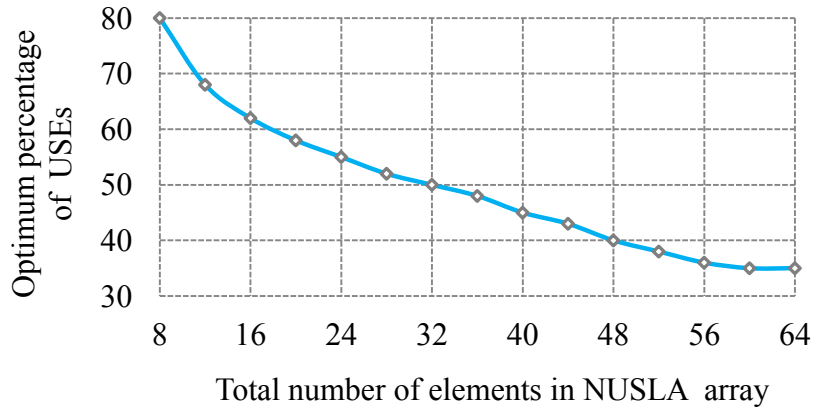


Fig. 2-29: Variation of optimum percentage of unequally spaced elements with total number of elements in NUSLA arrays.

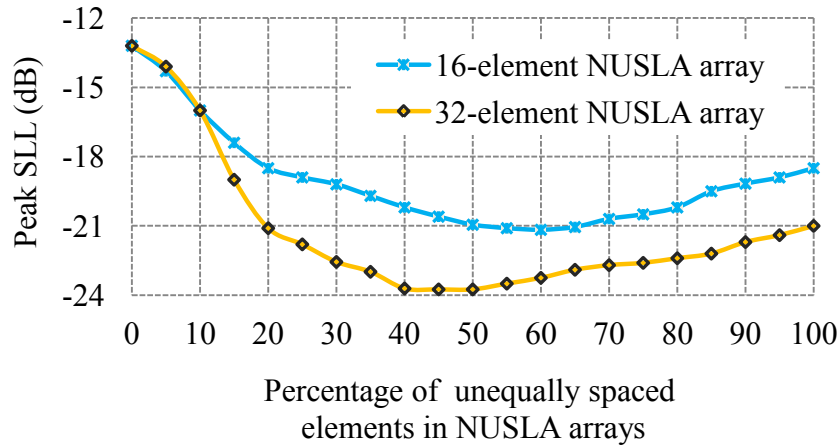


Fig. 2-30: Variations of peak SLL with percentage of unequally spaced elements for the proposed 16- and 32-elements NUSLA arrays.

This is associated with a particle size of 10 variables for rendering the desirable solution. The variation of the fitness value versus the number of iterations for the present study as well as for that reported in [Chen *et al.* (2006)] are shown in Fig. 2-31. The best fitness value i.e. minimum possible PSLL of -21.1 dB reaches within 15

iterations. The best array geometry obtained by IW-PSO algorithm with the aforementioned settings is listed in Table 2-16. The corresponding synthesized elements' density taper resembles the conventional Taylor taper as depicted in Fig. 2-32. The radiation pattern obtained through the proposed method for 16-element array is illustrated in Fig. 2-33 and values of PSLL determined using the proposed method and those using MGA [Chen *et al.* (2006)], SaDE [Goudos *et al.* (2011)], and SPSA [Lin *et al.* (2012)] are listed in Table 2-17. It can be observed from Fig. 2-33 and Table 2-17 that the PSLL obtained through the proposed method is -21.1 dB, which is 1.3 dB, 1.2 dB and 1.1 dB lower than those obtained in [Chen *et al.* (2006)], [Goudos *et al.* (2011)], and [Lin *et al.* (2012)] respectively. Total number of computations required till the convergence in the proposed method is 1×10^5 , however it is 8×10^5 in [Chen *et al.* (2006)] which shows that proposed method is 87% more efficient than MGA reported in [Chen *et al.* (2006)].

In the second example of 32-elements NUSLA array, basic parameters of evolving process were same as those of the previous one. The optimum percentage of unequally spaced elements was opted to be 50% of total number of elements as formulated in Eq. (2.18) and given in Fig. 2-29 which is related to a particle of 16 variables for yielding the optimal solution. The variation of best fitness value measured by side lobe level as a function of iteration number is shown in Fig. 2-34. It can be seen from Fig. 2-34 that the fitness function value reaches its best possible value i.e. minimum possible SLL of -23.7 dB within 25 iterations. The saturation of fitness value in the present case implies fast convergence as compared to the method presented in [Goudos *et al.* (2010)]. The best array geometry obtained by proposed technique with the aforementioned settings is listed in Table 2-16. Comparison of synthesized elements' density taper with corresponding Taylor taper is shown in Fig. 2-35. It can be observed from Fig. 2-35 that synthesized taper almost resembles the Taylor taper with a

difference that in central region of synthesized taper, 50% of the total number of array elements are equally spaced.

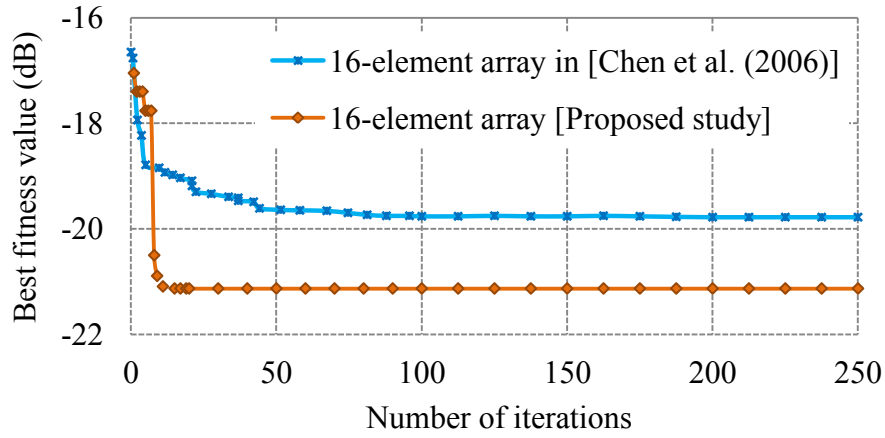


Fig. 2-31: Variations of best fitness value with number of iterations for the proposed 16-element NUSLA array and that published in [Chen *et al.* (2006)].

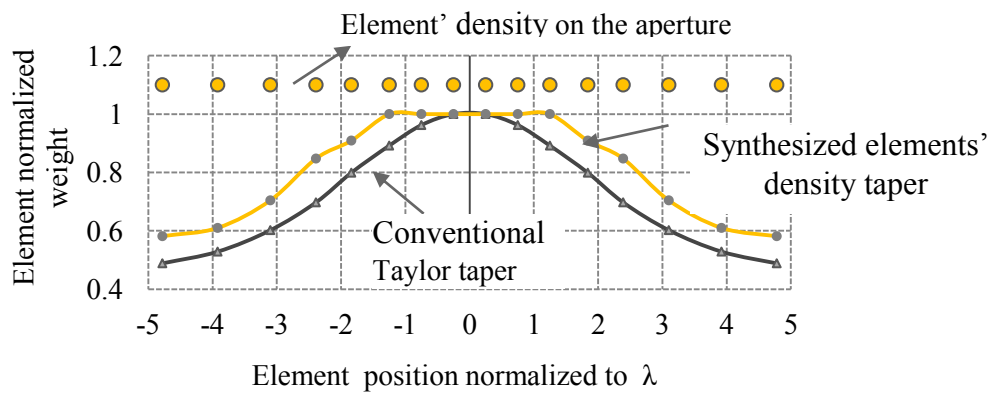


Fig. 2-32: Comparison of synthesized elements' density taper with the corresponding Taylor taper for the proposed 16-element NUSLA array.

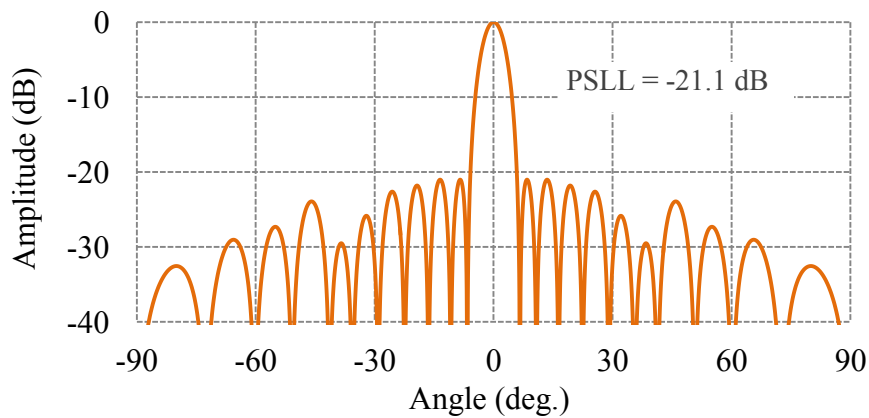


Fig. 2-33: Normalized radiation pattern of the proposed 16-element NUSLA array.

The radiation pattern of the proposed 32-element NUSLA array is depicted in Fig. 2-36. Table 2-17 compares the results obtained for the proposed NUSLA array and those for the arrays reported in literature [Goudos *et al.* (2010)], [Lin *et al.* (2010)], and [Zhang *et al.* (2013)]. The numerical results demonstrate that the proposed method offers more than 1 dB improvement in terms of PSLR suppression and the involved computational cost is 15% less as compared to respective parameter values reported in [Goudos *et al.* (2010)]. As compared to the existing arrays reported in [Chen *et al.* (2006)], [Goudos *et al.* (2010)], [Lin *et al.* (2010)], [Goudos *et al.* (2011)], [Lin *et al.* (2012)], and [Zhang *et al.* (2013)], lower PSLR is obtained with less computational complexity using the proposed approach.

Table 2-16: Geometry of the best array obtained for half of the proposed 16- and 32-elements NUSLA arrays normalized to free space wavelength.

N=16	0.25	0.50	0.50	0.59	0.55	0.71	0.82	0.86
N=32	0.25	0.50	0.50	0.50	0.50	0.50	0.50	0.50
	0.62	0.74	0.68	0.70	0.82	0.88	0.92	1.31

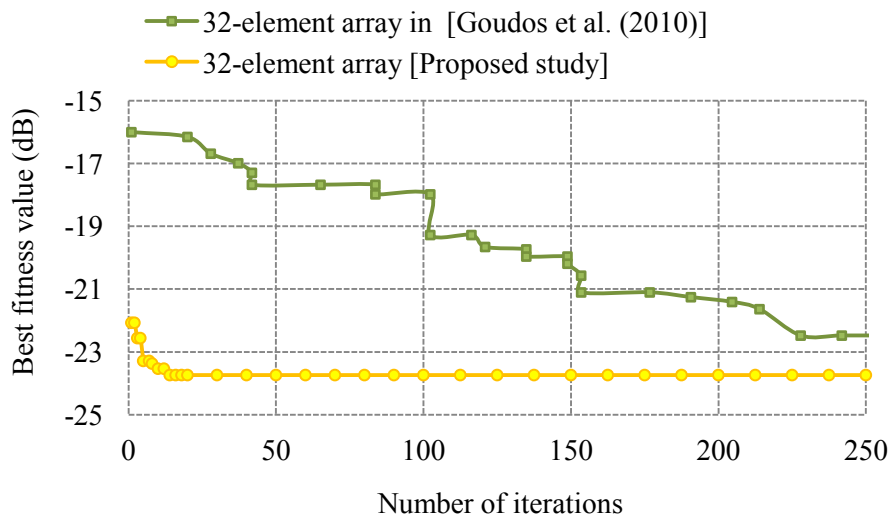


Fig. 2-34: Variations of best fitness values with number of iterations for the proposed 32-element NUSLA array and that published in [Goudos *et al.* (2010)].

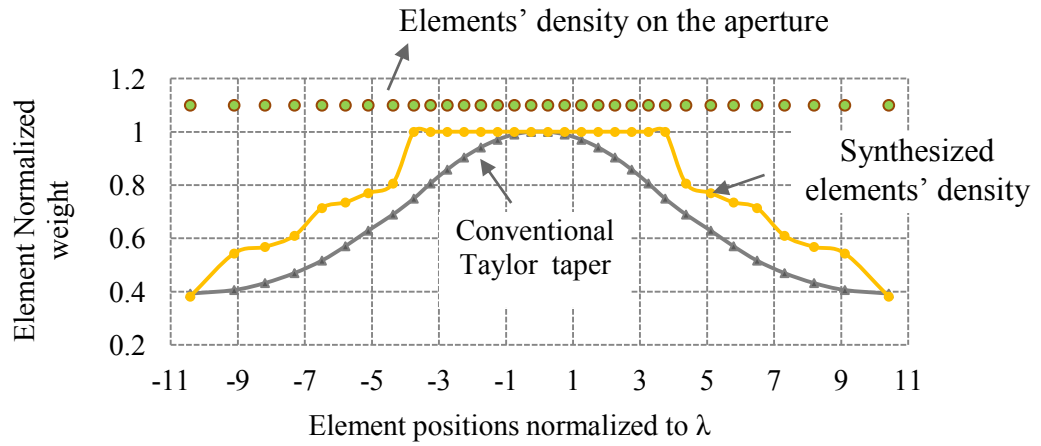


Fig. 2-35: Comparison of synthesized elements' density taper with the corresponding Taylor taper for the proposed 32-elements NUSLA array.

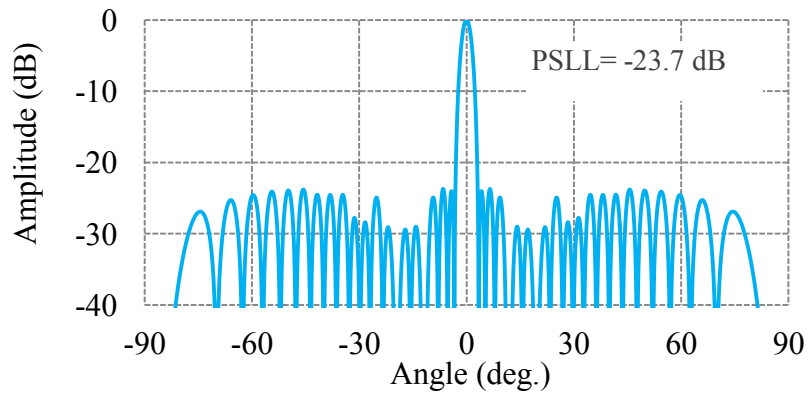


Fig. 2-36: Normalized radiation pattern of the proposed 32-element NUSLA array.

Table 2-17: Comparison of PSLL for the proposed NUSLA arrays with those published in [Chen *et al.* (2006)], [Goudos *et al.* (2010)], [Lin *et al.* (2010)], [Goudos *et al.* (2011)], [Lin *et al.* (2012)], and [Zhang *et al.* (2013)].

N=16	Parameter	MGA [Chen <i>et al.</i> (2006)]	SaDE [Goudos <i>et al.</i> (2011)]	SPSA [Lin <i>et al.</i> (2012)]	IW-PSO [Proposed]
	Peak SLL (dB)	-19.79	-19.89	-19.98	-21.10
N=32	Parameter	CLPSO [Goudos <i>et al.</i> (2010)]	DE [Lin <i>et al.</i> (2010)]	HSDA [Zhang <i>et al.</i> (2013)]	IW-PSO [Proposed]
	Peak SLL (dB)	-22.75	-22.65	-22.63	-23.70

2.3.4.3 PSL Optimization at Boresight as well as upto $\pm 30^\circ$ Scan Angles in 16-element NUSLA Array using PSO

The effectiveness of the proposed algorithm is assessed by analysing a NUSLA array with 16 sources symmetrically placed with unequal spacing along the X-axis with the centre at the origin. The uniform amplitude excitations and zero phases across all the elements in array are considered. Due to symmetry in the array, only half of the array is considered for optimization, which reduces the computational effort of optimization algorithm. As optimization constraints, inter-element spacings were chosen in the range $0.5\lambda - 1.5\lambda$. Under this constraint, PSO algorithm was applied with an initial random population of 1000 particles and iterated for 500 iterations. The algorithm parameters c_1 and c_2 were set to values of 1 and 3, $r_{1,i}$ and $r_{2,i}$ were set to values of 0.3 and 0.7 during search for an optimum solution. The variation of the PSL value versus the number of iterations for the proposed study is depicted in Fig. 2-37. The best fitness value i.e. minimum possible SLL of -17.4 dB reaches within less than 370 iterations. The element positions of the best array geometry obtained by PSO algorithm with the aforementioned settings is listed in Table 2-18. The comparisons of the radiation patterns of the proposed 16-element NUSLA array with those of uniformly excited array at antenna boresight, and 30° scan angles with respect to antenna boresight are shown in Figs. 2-46 and 2-47 respectively. The radiation characteristics extracted from Figs. 2-46 and 2-47 are tabulated in Table 2-19. It can be observed from Figs. 2-38, 2-39 and Table 2-19 that the PSL at 30° scan angle is almost the same as at boresight. These patterns demonstrate that the optimized NUSLA array has a much larger scan range than its periodic counterparts. The appearance of grating lobes during the array scanning has an adverse affect on the peak gain of the antenna system. When a grating

lobe appears, a good amount of energy is taken away from the main beam and directed into the grating lobe resulting in a reduction in gain of antenna system. This evidenced that proposed PSO based optimization technique has great potential to optimize NUSLA arrays over the pre-specified scan volume required for electronically scanned radar applications.

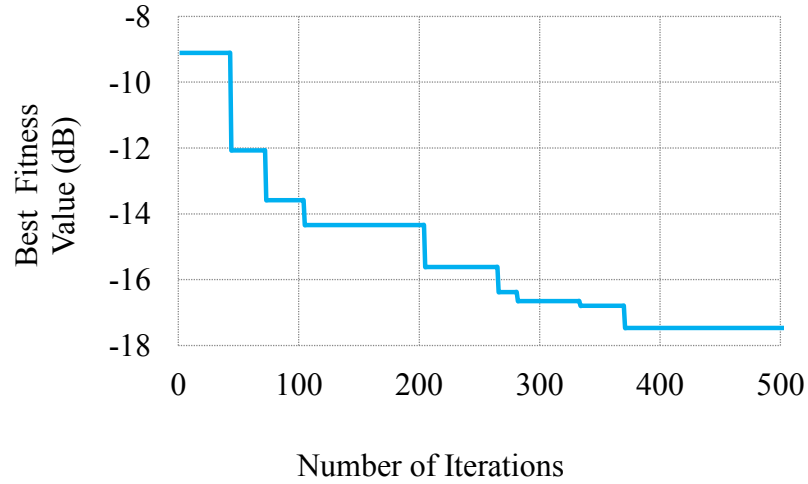


Fig. 2-37: Variation of best fitness value i.e. PSL with number of iterations for the proposed 16- element NUSLA array.

Table 2-18: Geometry of the array positions obtained by the proposed PSO based method.

Element number	Inter-element spacing normalised to λ	Element number	Inter-element spacing normalised to λ
1	0	9	3.69
2	0.55	10	3.99
3	1.07	11	4.3
4	1.57	12	4.79
5	2.08	13	5.29
6	2.56	14	5.8
7	2.87	15	6.31
8	3.18	16	6.86

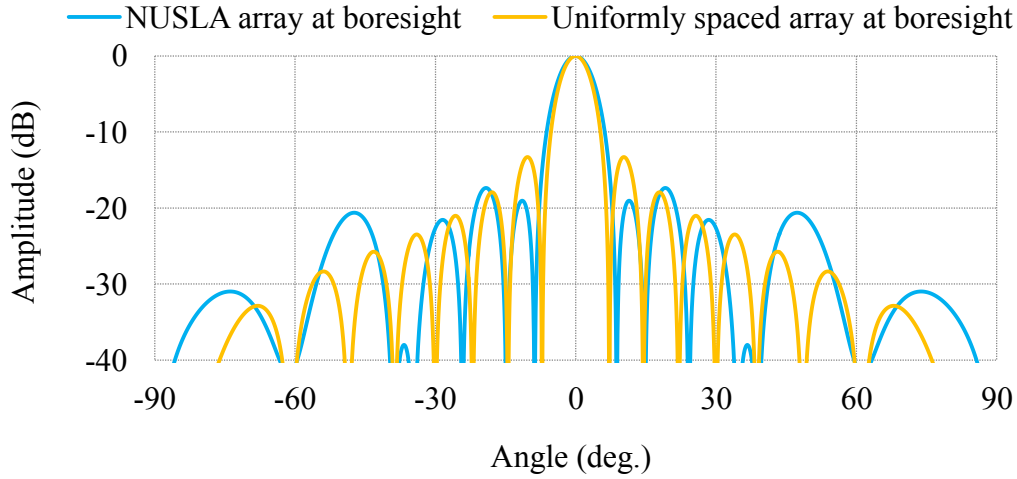


Fig. 2-38: Comparison of radiation pattern of the proposed 16-element NUSLA array with that of the uniformly spaced array at boresight.

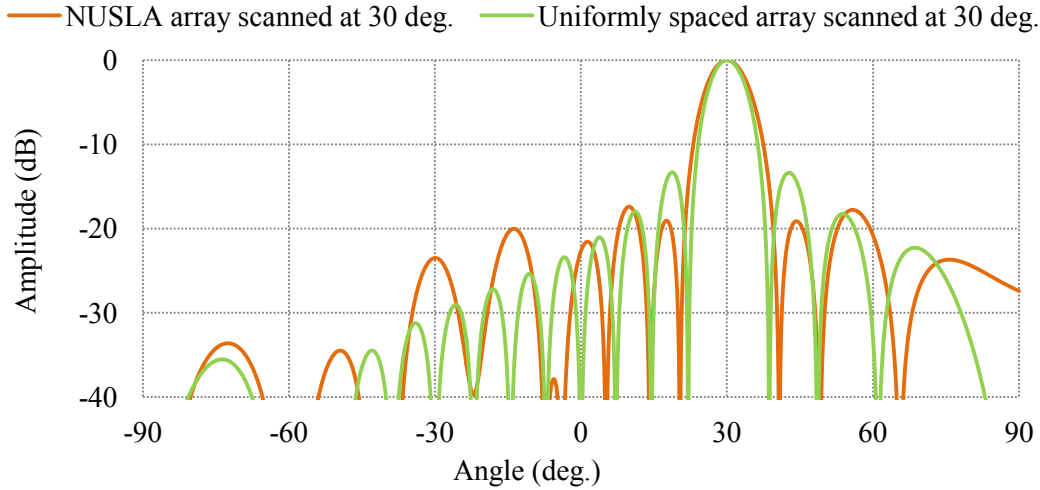


Fig. 2-39: Comparison of radiation pattern of the proposed 16-element NUSLA array with that of the uniformly spaced array when both are steered at 30° scan angle with respect to antenna boresight.

Table 2-19: Comparison of PSL performance obtained through the proposed 16-element NUSLA array with those of uniformly spaced array of same size.

Scan angle	PSLL (dB) uniformly spaced array	PSLL (dB) NUSLA array
0°	-13.38	-17.46
30°	-13.38	-17.41

2.3.4.4 Optimization of PSLL in Uniformly Excited and Amplitude Weighted 36-element NUSLA Array Using PSO

The optimum inter-element spacings and amplitude coefficients obtained by proposed method for half of the array are listed in Table 2-20, and corresponding geometry with dimensions at a frequency of 9.5 GHz is depicted in Fig. 2-40. The convergence of the fitness value versus the number of iterations is shown in Fig. 2-41. The array radiation patterns of the geometry shown in Fig. 2-41 for both spacing only (SO) and SA spacing and amplitude syntheses are demonstrated in Fig. 2-42. The array parameters extracted from Fig. 2-42 are listed in Table 2-21 and compared with those obtained using the optimization techniques reported in [Chen *et al.* (2006)], [Zhang *et al.* (2011)] for SO synthesis, in [Lin *et al.* (2010)], [Cen *et al.* (2012)] for both spacing phase (SP) and SA syntheses and with those determined for similar size uniform array employing amplitude only (AO) synthesis. It can be noticed from Table 2-21 that the PSLs for the array are -23.28 dB and -30.27 dB for SO and SA syntheses respectively which are lower by 0.65 to 2.72 dB than the best PSL obtained in [Chen *et al.* (2006)], [Lin *et al.* (2010)], [Zhang *et al.* (2011)], and [Cen *et al.* (2012)] for SO synthesis lower by 6.18 dB than the best PSL obtained in [Lin *et al.* (2010)] for SP synthesis, and by 7.97 dB obtained in [Cen *et al.* (2012)] for SA synthesis while maintaining almost equal HPBW and directivity.

Table 2-20: Optimum combinations of inter-element spacing and amplitude excitations for half of the proposed 36-element NUSLA array.

Inter-element spacing	0.25	0.50	0.50	0.50	0.50	0.50	0.50	0.50	0.70
normalized to λ	0.64	0.48	0.63	0.83	0.87	0.89	0.85	1.03	1.19
Amplitude excitation	1.0	1.0	1.0	1.0	1.0	1.0	1.0	1.0	0.91
coefficients	0.83	0.61	0.92	0.89	0.70	0.56	0.50	0.28	0.06

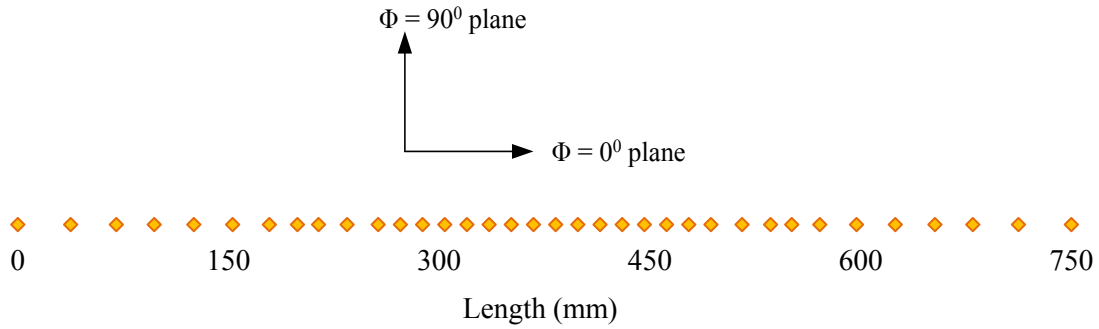


Fig. 2-40: Proposed geometry of 36-element NUSLA array with dimensions corresponding to a frequency of 9.5 GHz.

There is reduction of 0.6 deg in HPBW and improvement of 0.9 dB in directivity for the proposed array as compared with the corresponding Taylor amplitude (TA)-tapered uniform array of similar size

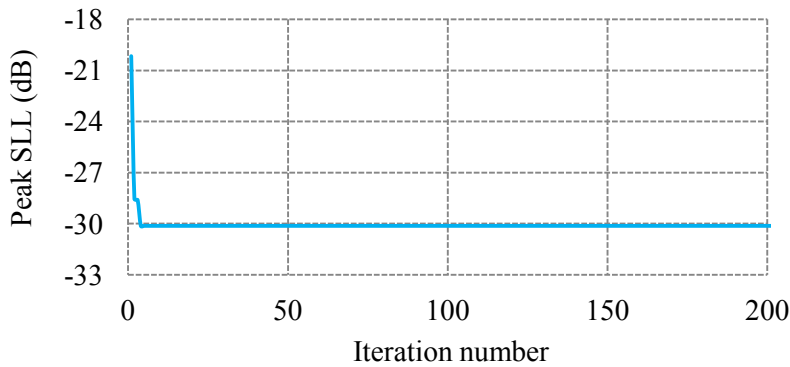


Fig. 2-41: Peak SLL vs. number of iterations for the SA synthesis of the proposed 36-element NUSLA array.

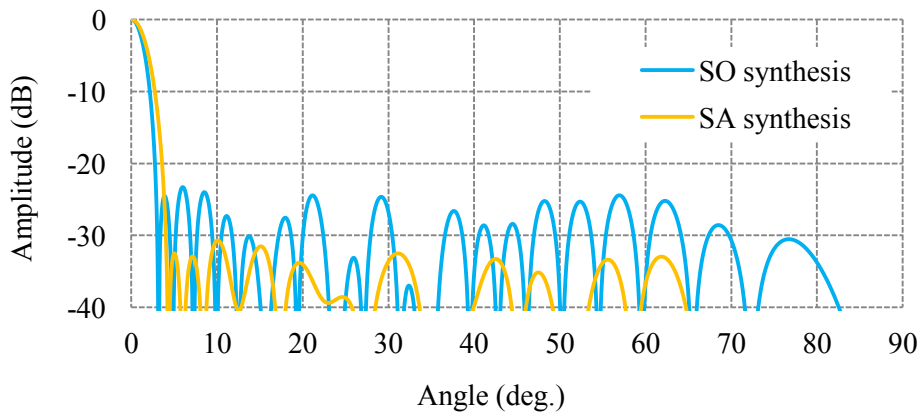


Fig. 2-42: Numerically evaluated radiation patterns of the proposed 36-element NUSLA array.

Table 2-21: Comparison of numerically evaluated results for the proposed NUSLA array with those for uniformly spaced array and the results published in literature [Chen *et al.* (2006)], [Lin *et al.* (2010)], [Zhang *et al.* (2011)] and [Cen *et al.* (2012)] .

Design parameters		Uniformly spaced array	MGA [Chen <i>et al.</i> (2006)]	SHDE [Zhang <i>et al.</i> (2011)]	DE [Lin <i>et al.</i> (2010)]	IGA [Cen <i>et al.</i> (2012)]	PSO [Proposed]
Percentage of unequally spaced elements		-	100	100	100	100	55
Aperture size (λ)		24	21.99	24.23	24.23	25	23.75
PSLL (dB)	TA	-30	-	-	-	-	-
	SO	-	-20.56	-22.63	-22.62	-22.40	-23.28
	SP	-	-	-	-24.11	-	-
	SA	-	-	-	-	-22.3	-30.27
HPBW (deg)	TA	4					-
	SO	-		2.818	2.814		2.822
	SP	-					-
	SA	-					3.4
Directivity (dB)	TA	13.85					-
	SO			15.8	15.8		15.78
	SP						-
	SA						14.75

2.3.5 EM Simulation and Experimental Validation of 24-element NUSLA Array

In the design of NUSLA for practical applications, it is very essential to consider the effect of mutual coupling among the array elements because it can impact significantly the antenna input impedance, the array gain, and the SLL of the array pattern. But due to non existence of exact mathematical expression for evaluating the effect of mutual coupling and its explicit relationship with the array pattern, the analysis and design of

array are complicated. That's why, many array synthesis methods [Haupt (1995)], [Chen *et al.* (2006)], [Goudos *et al.* (2010)] and [Fuchs *et al.* (2012)], have not considered mutual coupling aspects while synthesizing the NUSLA arrays.

In proposed synthesis, the constraint for the inter-element spacing d_i to be $0.5\lambda \leq d_i \leq 1.5\lambda$ is adopted so that the average inter-element spacing in NUSLA array is relatively large with respect to equally-spaced arrays. This, in turn, conciliates the effect of mutual coupling among the radiating elements and results in simple analysis and design of NUSLA arrays.

In order to validate the performance of proposed method in presence of mutual coupling among elements, a NUSLA array with 24 equally-excited elements arranged as per spacings provided in Table 2-14 in numerical analysis section is simulated using HFSS/CST EM software. The M-shaped patch [Aggarwal and Gangwar (2014)], whose geometry and design parameters are reproduced in Fig. 2-43 and Table 2-22 respectively, considered as a radiating element in the simulation of the proposed NUSLA array. This antenna element provides minimum gain of 5.8 dB and 3-dB beam width of the order of 85° in both planes. Figure 2-52 shows EM simulation model of the NUSLA under study where with adopted inter-element spacings, the mutual coupling level among the radiating elements was found to be <-18 dB. Simulated radiation patterns of the proposed NUSLA array with mutual coupling effect in $\phi = 0^\circ$ plane are depicted in Figs. 2-53 and 2-54. The 3D radiation pattern of the proposed 24-element NUSLA array is shown in Fig. 2-48. The NUSLA array parameters are extracted from Figs. 2-53, 2-54 and 2-55 and the results are compiled in Table 2-23 along with the results published in [Caratelli and Vigano (2011)] in presence of mutual coupling effect. In spite of -18 dB mutual coupling, as it can be noticed from Figs. 2-53, 2-54 and 2-55

and Table 2-23, the radiation pattern of the NUSLA array is not very severely impacted, except for the first side lobe level which is degraded from -26.9 dB to -20.7 dB and gain by 0.68 dB. Additionally, It can be observed from the 3D radiation pattern shown in Fig. 2-48 that no lobe exist which is greater than first side-lobe in any plane of the Proposed NUSLA array. This means that the proposed synthesis method yields pretty optimistic results in realistic operating conditions where the effect of mutual coupling among array elements cannot be neglected.

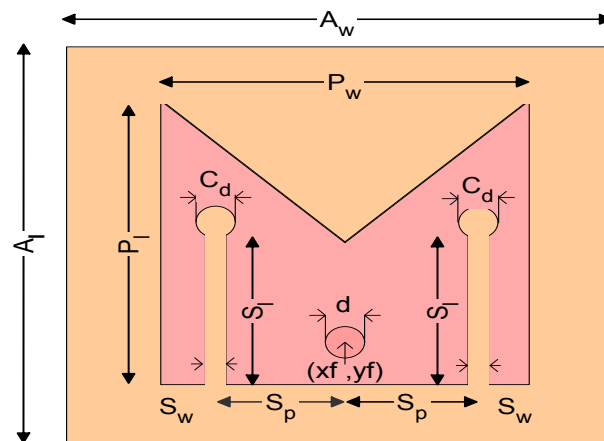


Fig. 2-43: The geometry of M-shaped patch radiating element [Aggarwal and Gangwar (2014)].

Table 2-22: Design parameters of the M-shaped patch antenna [Aggarwal and Gangwar (2014)].

Parameter	Value (mm)	Parameter	Value (mm)
A_l	14	S_p	4.5
A_w	14	C_d	0.6
P_l	9.1	d	0.6
P_w	9	D	1.28
S_l	5.7	(x_f, y_f)	(0, -2.45)
S_w	0.57		

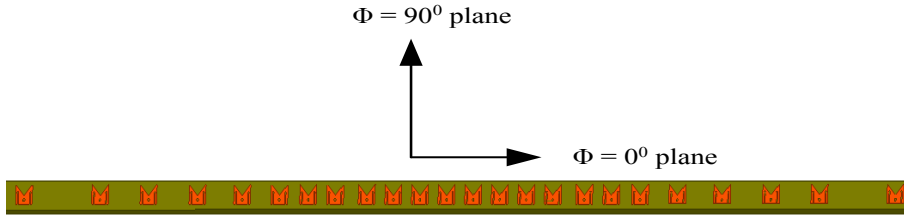


Fig. 2-44: EM Simulation model of the proposed 24-element NUSLA array.

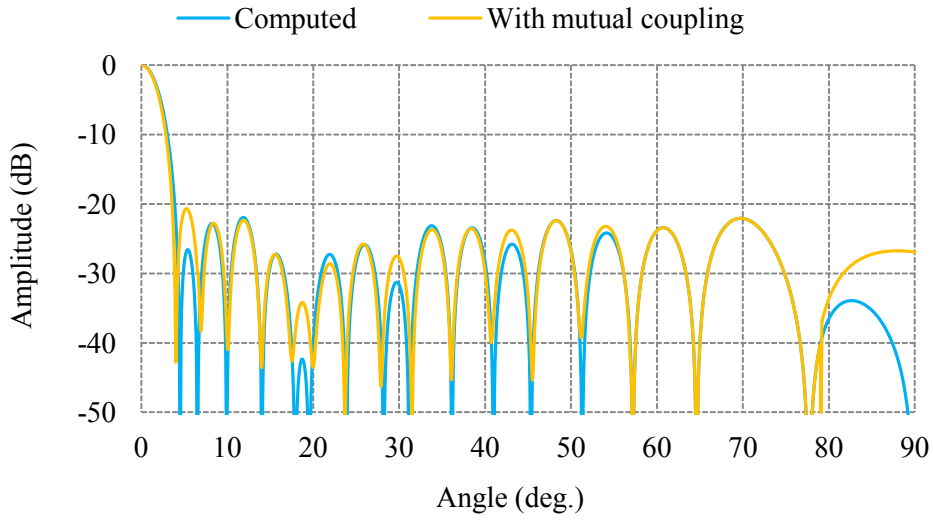


Fig. 2-45: Comparison of numerically evaluated radiation pattern with those for EM simulated of the proposed NUSLA array in $\phi = 0^\circ$ plane.

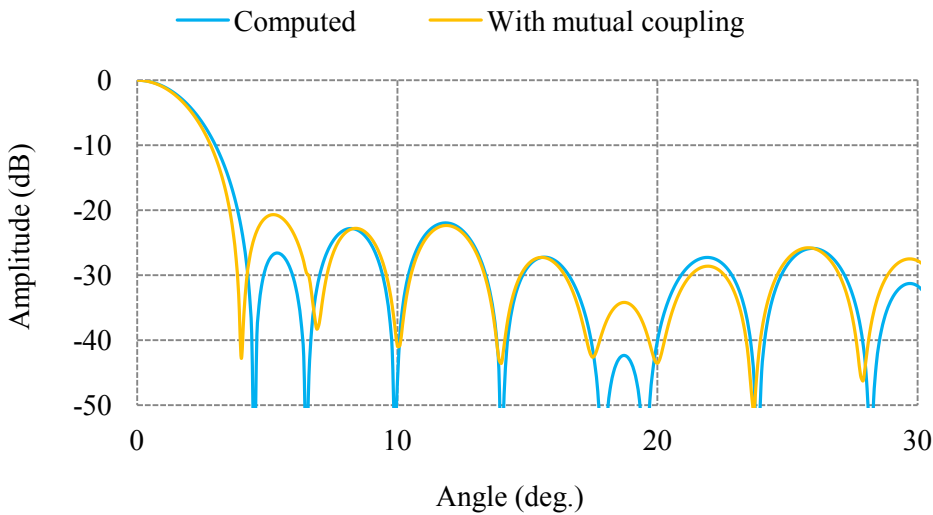


Fig. 2-46: Comparison of numerically evaluated radiation pattern with those for EM simulated of the proposed NUSLA array in $\phi = 0^\circ$ plane in the angular sector ($\theta = 0^\circ$ to 30°).

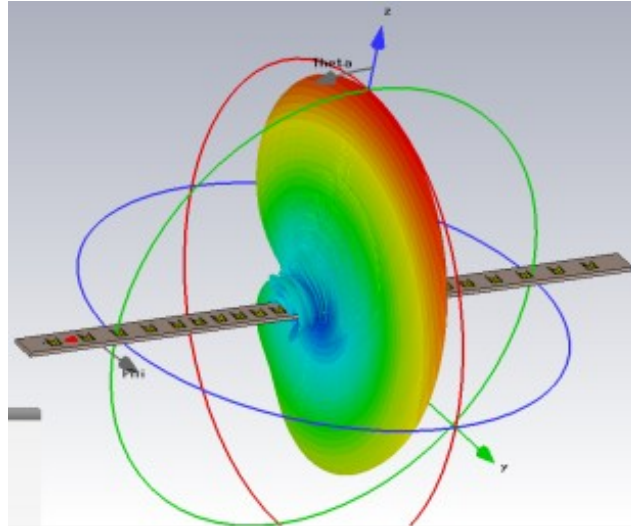


Fig. 2-47: 3D radiation pattern of the proposed 24-element NUSLA array.

Table 2-23: Comparison of simulated results for the proposed NUSLA array with and without mutual coupling and with those published in literature [Caratelli and Vigano (2011)].

Parameters	Without mutual coupling [Proposed]	With mutual coupling [Caratelli and Vigano (2011)]	With mutual coupling [Proposed]
PSLL (dB)	-22	-18	-20.7
HPBW (deg)	3.49	5.68	3.30
Directivity (dB)	20.84	-	20.16

The proposed NUSLA array with the synthesized inter-element spacings was fabricated, integrated and tested. The realized NUSLA array was integrated with 1:24 equal way feed network (not a part of present work) through 24 equi-phase cables as shown in Fig. 2-48. Measurement of radiation pattern of the array was carried out in Planar Near Field Test Range (NFTR). The near field data (amplitude and phase) were measured as shown in Fig. 2-49, by scanning probe over a pre-defined plane surface and measured data were then transformed to far-field as shown in Fig. 2-50 using analytical

Fourier transform method. Acquisition and analysis of near field data were done by data acquisition and analysis software. The antenna array under test was held stationary while the probe (open-ended waveguide) was moved to each grid location in the plane.

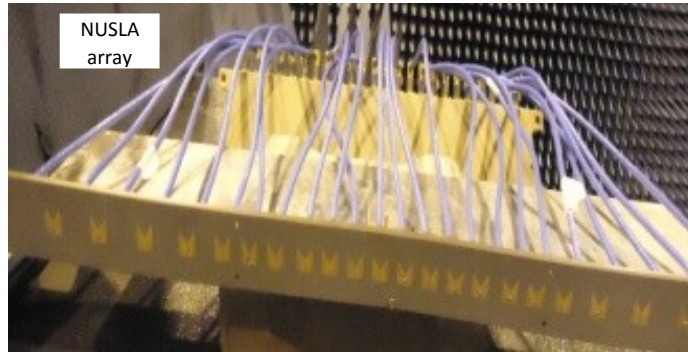


Fig. 2-48: Realized 24-element NUSLA array intergrated with feed network.

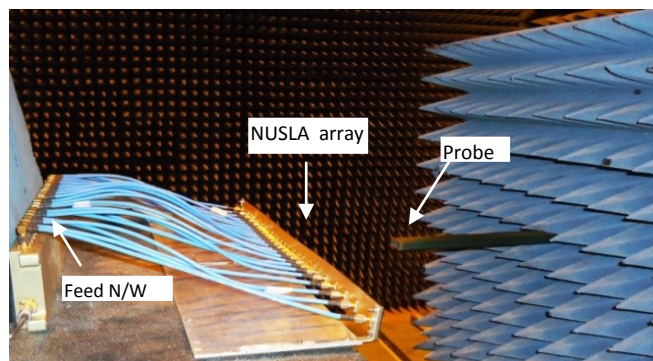


Fig. 2-49: Realized NUSLA array under pattern measurement in NFTR.

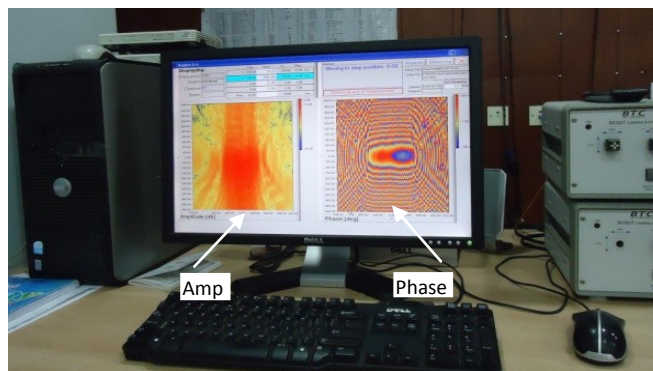


Fig. 2-50: Sampled near field amplitude and phase of the proposed NUSLA array during pattern measurement.

Comparison of measured and simulated radiation patterns of the array is shown in Fig. 2-51 and the parameters extracted from Fig 2-51 are listed in Table 2-24. It can be observed from Table 2-24 that simulated and measured results are in close agreement.

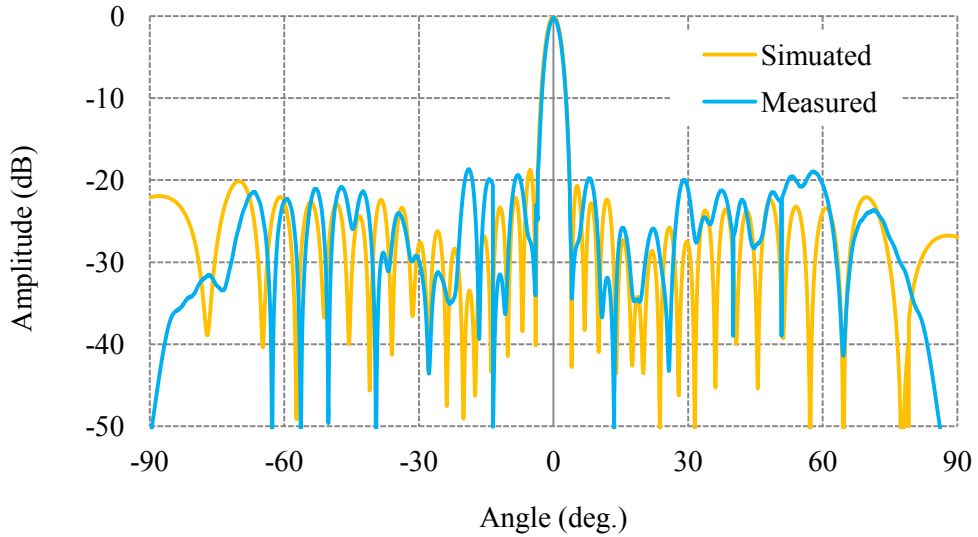


Fig. 2-51: Comparison of simulated and measured radiation patterns of the proposed 24-element NUSLA array.

Table 2-24: Comparison of simulated and measured results for the proposed 24-element NUSLA array and with simulated ones published in literature [Caratelli and Vigano (2011)].

Parameters	Simulated			Measured
	Without mutual coupling [Proposed]	With mutual coupling [Caratelli and Vigano (2011)]	With mutual coupling [Proposed]	[Proposed]
Peak SLL (dB)	-22	-18	-20.7	-19.8
Beam width (deg)	3.49	5.68	3.30	-3.38
Directivity (dB)	20.84	-	20.16	19.8

2.4 Summary and Conclusion

In this chapter, implementation of various synthesis methods for the design of sparse linear antenna (TLA and NUSLA) arrays based on GA and PSO optimization techniques have been demonstrated. The performance and capability of presented synthesis methods have been evaluated by numerically analysing different examples of TLA and NUSLA arrays. In addition, EM simulation and experimental validation have also been done on a 24-element NUSLA array to further affirm the performance in practical scenario.

From the numerical analysis of various examples described in this chapter, it is clear that the proposed methods exhibit the following characteristics:

- Better performance in suppression of PSLL at antenna boresight with minimum number of turn 'ON' elements
- Reduction of PSLL at antenna boresight as well as over the pre-specified scan volume
- Joint optimization of PSLL, HPBW and gain or directivity.
- The afore-mentioned characteristics have been achieved at less computational complexity and great stability as compared to those associated with the existing state-of-the-art methods.

Similarly, the proposed synthesis approaches presented for NUSLA arrays offer better PSLL suppression as compared to the synthesis techniques reported in the literature.

In addition, the results show that the simulated radiation pattern of the NUSLA array has not been severely impacted due to mutual coupling between the array elements. This means that the proposed synthesis method yields moderately optimistic results in practical operating scenario where the effect of mutual coupling cannot be ignored.